

Electronic Supporting Information (ESI)

Phosphorus guiding palladium: [4+4] metallomacrocyclic Pd^{II} complex and self-assembly of heterometallic Pd^{II}/Zn^{II} grid-type complex

Reike Clauss and Evamarie Hey-Hawkins

Faculty of Chemistry and Mineralogy, Institute of Inorganic Chemistry, Johannisallee 29, 04103 Leipzig, Germany

Table of Content

1. NMR Spectra (¹ H, ¹³ C{ ¹ H}, ¹⁹ F{ ¹ H}, ³¹ P{ ¹ H}, ¹ H- ¹ H COSY, ¹ H- ¹³ C HMBC, ¹ H- ¹³ C HSQC, ¹ H- ¹ H NOESY) of 2	2
2. NMR Spectra (¹ H, ¹³ C{ ¹ H}, ¹⁹ F{ ¹ H}, ³¹ P{ ¹ H}, ¹ H- ¹ H COSY, ¹ H- ¹³ C HMBC, ¹ H- ¹³ C HSQC, ¹ H- ¹ H NOESY) of 3	5
3. NMR Spectra (¹ H, ¹³ C{ ¹ H}, ¹⁹ F{ ¹ H}, ³¹ P{ ¹ H}, ¹ H- ¹ H COSY, ¹ H- ¹³ C HMBC, ¹ H- ¹³ C HSQC) of 4	9
4. NMR Spectra (¹ H, ¹³ C{ ¹ H}, ¹⁹ F{ ¹ H}, ³¹ P{ ¹ H}, ¹ H- ¹ H COSY, ¹ H- ¹³ C HMBC, ¹ H- ¹³ C HSQC, ¹ H- ¹ H NOESY) of 5	14
5. NMR Spectra (¹ H, ¹³ C{ ¹ H}, ¹⁹ F{ ¹ H}, ³¹ P{ ¹ H}, ¹ H- ¹ H COSY, ¹ H- ¹³ C HMBC, ¹ H- ¹³ C HSQC, ¹ H- ¹ H NOESY) of 6	17
6. NMR Spectra (¹ H, ¹³ C{ ¹ H}, ¹⁹ F{ ¹ H}, ³¹ P{ ¹ H}, ¹ H- ¹ H COSY, ¹ H- ¹³ C HMBC, ¹ H- ¹³ C HSQC, ¹ H- ¹ H NOESY) of 7	21
7. VT NMR Spectra (¹ H, ³¹ P{ ¹ H}) of 4 and 7	25
8. Reaction NMR Spectra	28
9. ¹ H DOSY NMR Spectra of Complexes 2–7	31
10. Mass Spectrometry	34
11. UV/Vis Spectroscopy	37
12. Additional Information on X-Ray Diffraction Analyses	39

1. NMR Spectra (^1H , $^{13}\text{C}\{^1\text{H}\}$, $^{19}\text{F}\{^1\text{H}\}$, $^{31}\text{P}\{^1\text{H}\}$, ^1H - ^1H COSY, ^1H - ^{13}C HMBC, ^1H - ^{13}C HSQC, ^1H - ^1H NOESY) of **2**

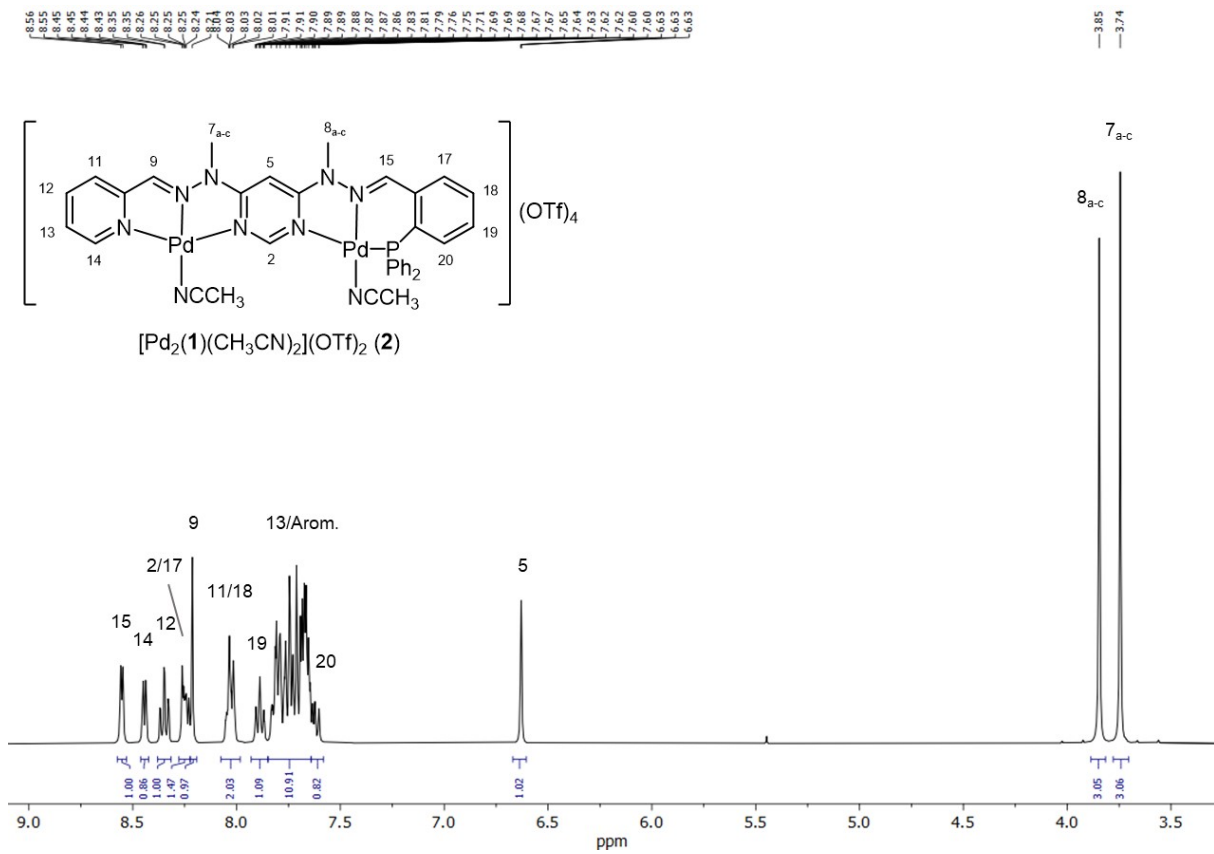


Figure S1. ^1H NMR spectrum of **2** in CD_3CN at 25 °C.

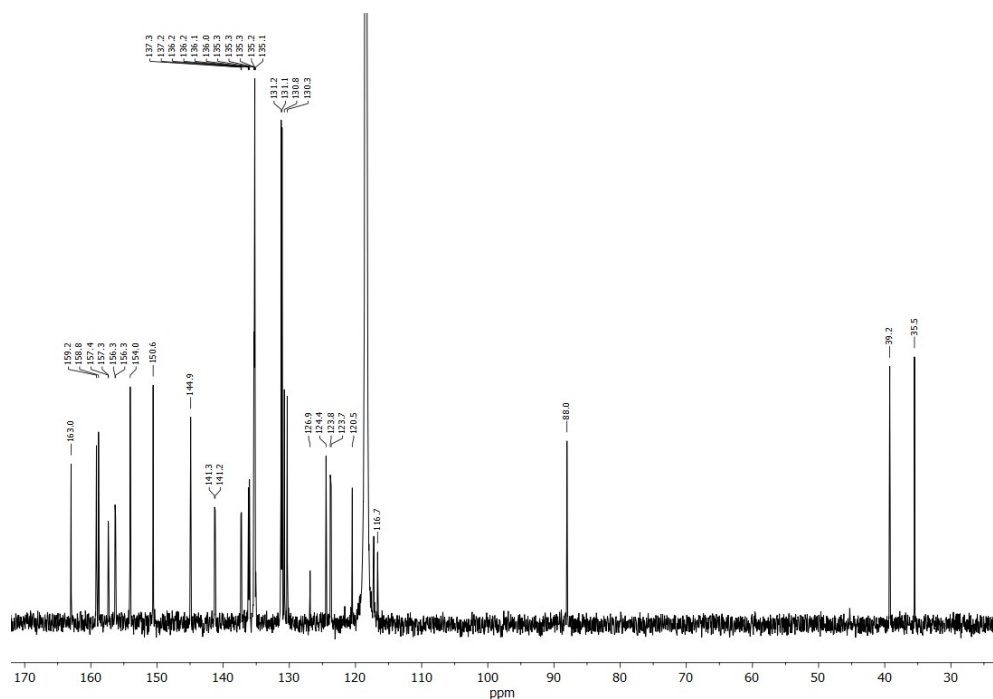


Figure S2. $^{13}\text{C}\{\text{H}\}$ NMR spectrum of **2** in CD_3CN at 25 °C.

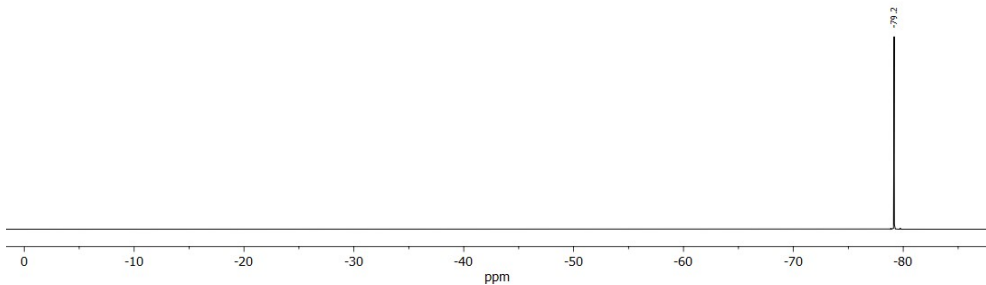


Figure S3. $^{19}\text{F}\{\text{H}\}$ NMR spectrum of **2** in CD_3CN at $25\text{ }^\circ\text{C}$.

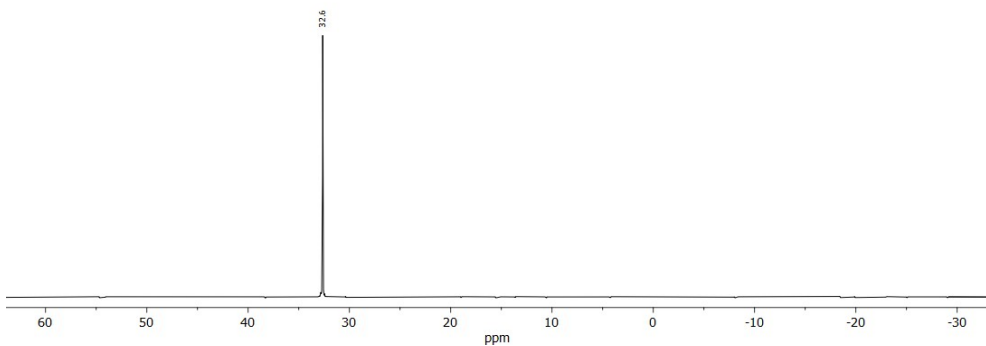


Figure S4. $^{31}\text{P}\{\text{H}\}$ NMR spectrum of **2** in CD_3CN at $25\text{ }^\circ\text{C}$.

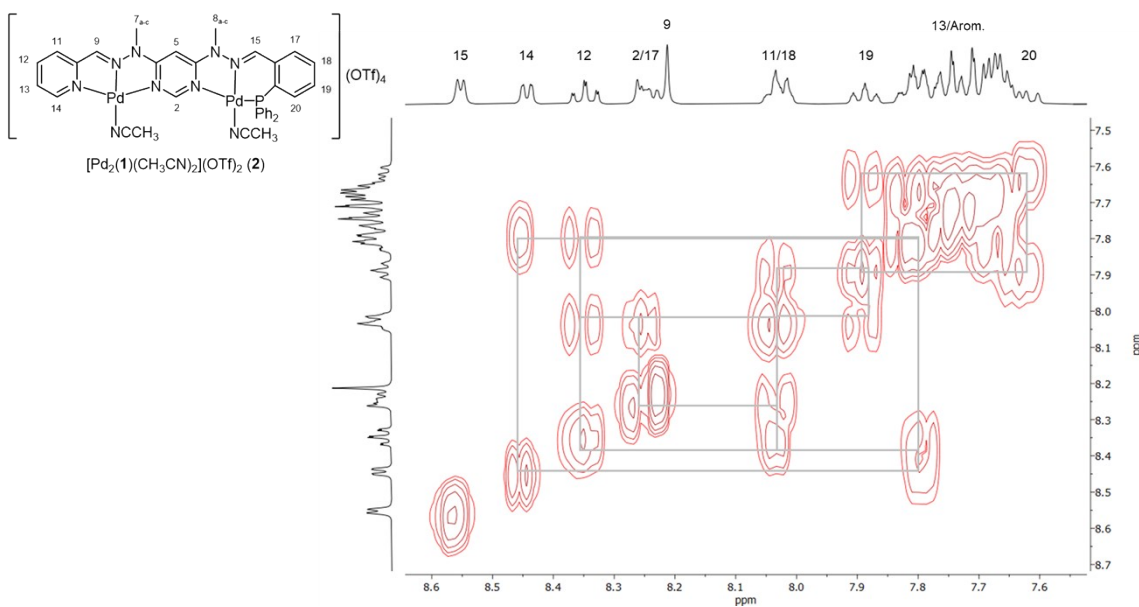


Figure S5. ^1H - ^1H COSY spectrum of **2** in CD_3CN at $25\text{ }^\circ\text{C}$.

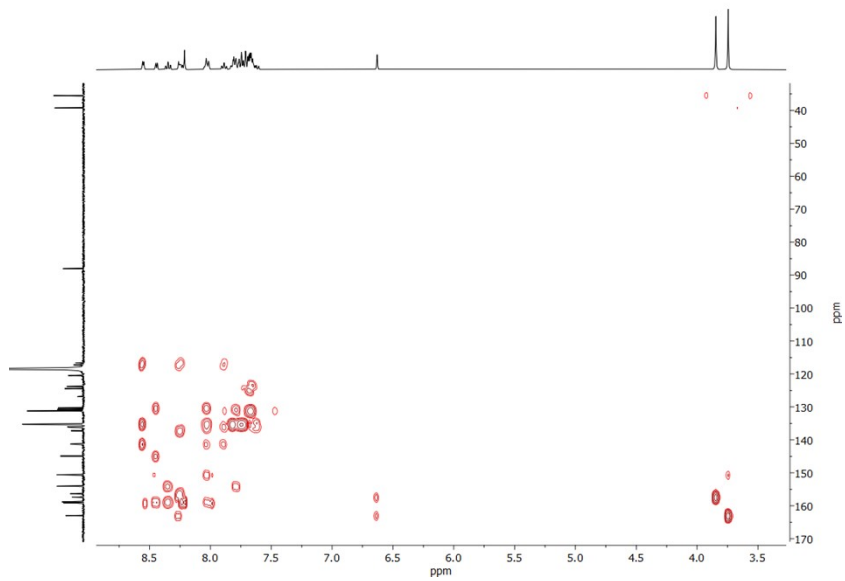


Figure S6. ¹H-¹³C HMBC spectrum of **2** in CD₃CN at 25 °C.

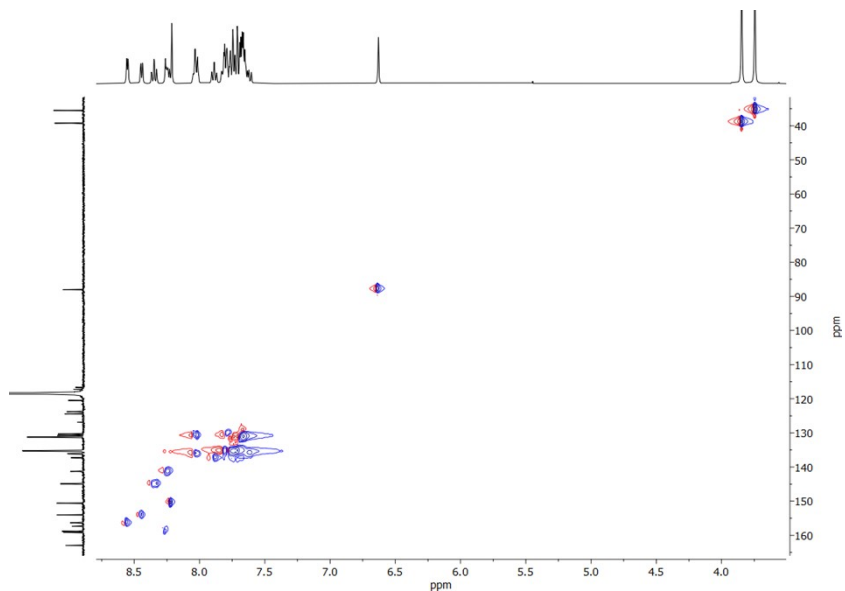


Figure S7. ¹H-¹³C HSQC spectrum of **2** in CD₃CN at 25 °C.

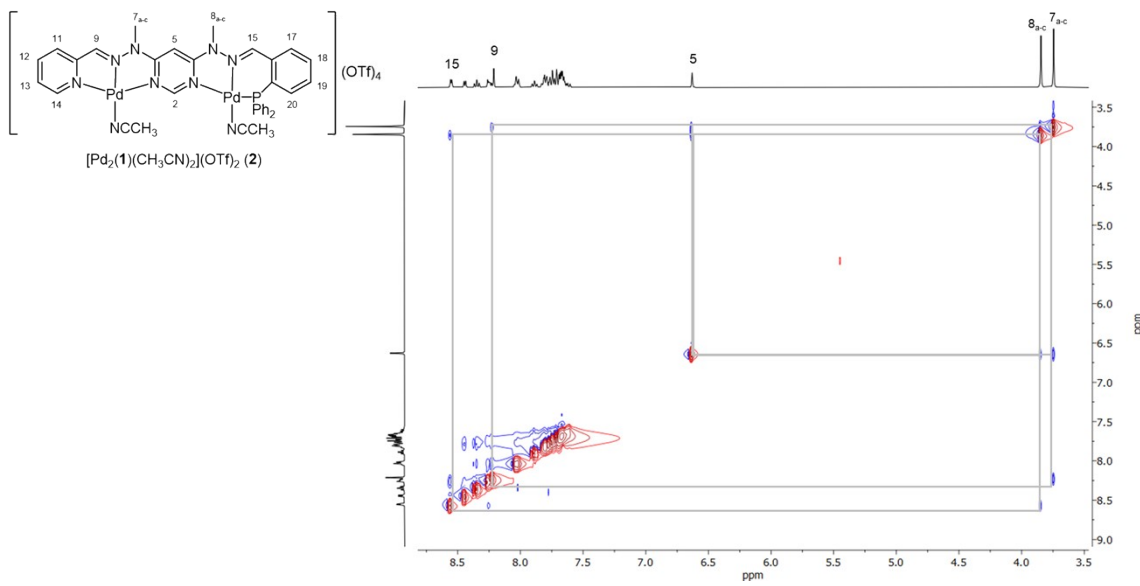


Figure S8. ^1H - ^1H NOESY spectrum of **2** in CD_3CN at 25 °C.

2. NMR Spectra (^1H , $^{13}\text{C}\{\text{H}\}$, $^{19}\text{F}\{\text{H}\}$, $^{31}\text{P}\{\text{H}\}$, ^1H - ^1H COSY, ^1H - ^{13}C HMBC, ^1H - ^{13}C HSQC, ^1H - ^1H NOESY) of **3**

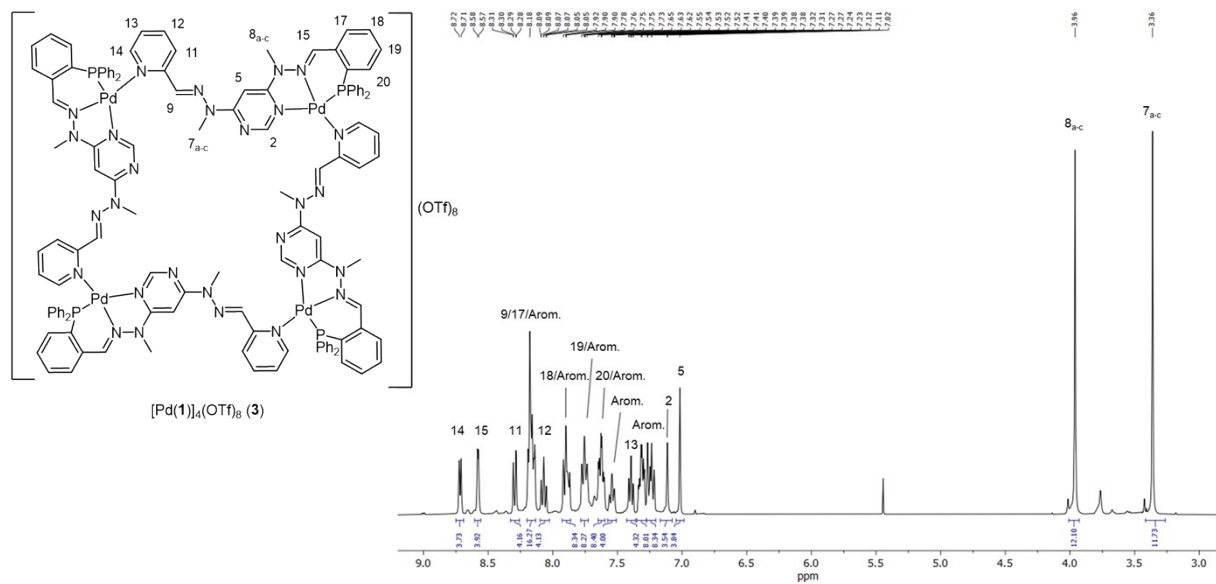


Figure S9. ^1H NMR spectrum of **3** in CD_3CN at 25 °C.

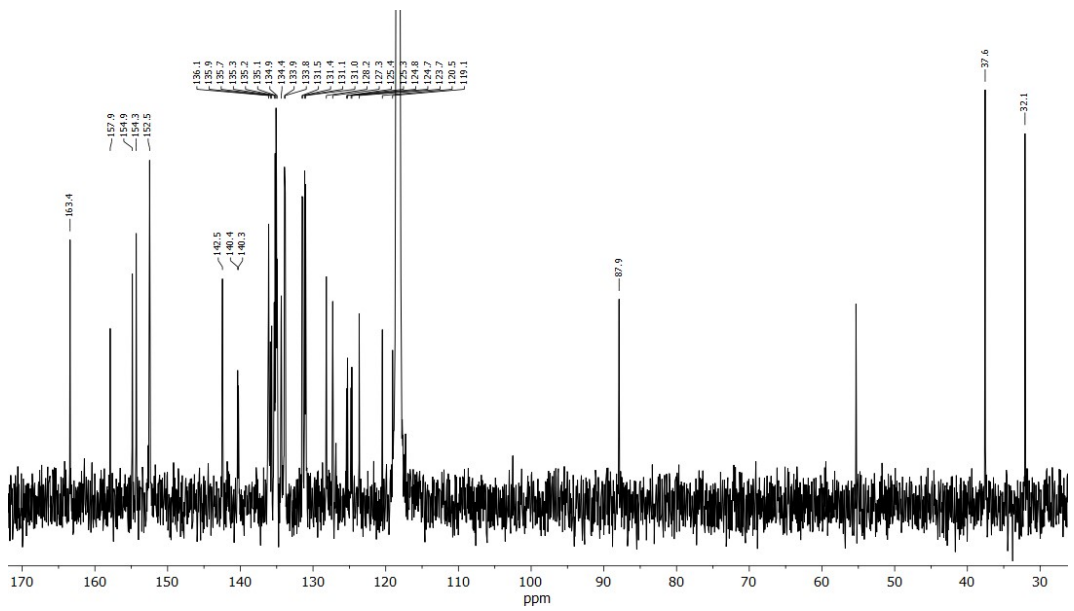


Figure S10. $^{13}\text{C}\{^1\text{H}\}$ NMR spectrum of **3** in CD_3CN at 25 °C.

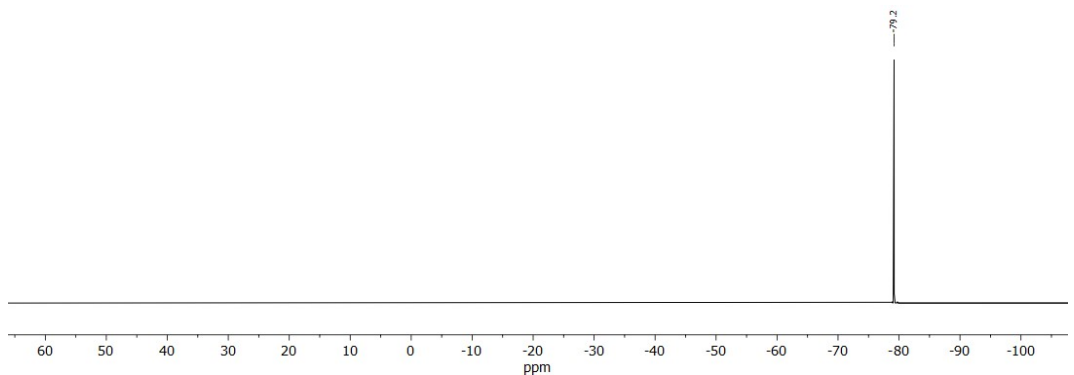


Figure S11. $^{19}\text{F}\{^1\text{H}\}$ NMR spectrum of **3** in CD_3CN at 25 °C.

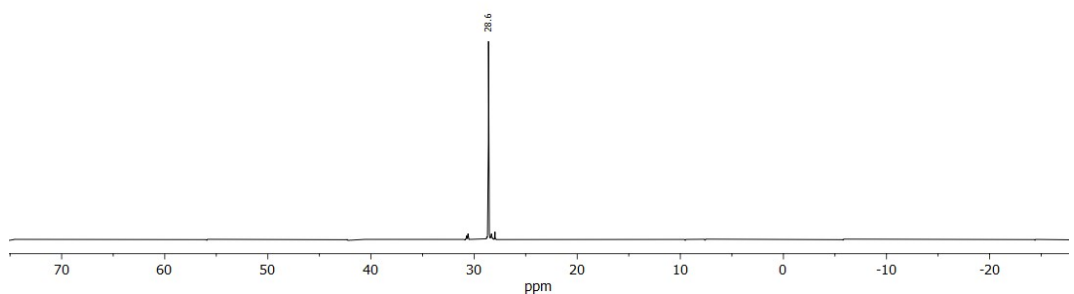


Figure S12. $^{31}\text{P}\{^1\text{H}\}$ NMR spectrum of **3** in CD_3CN at 25 °C.

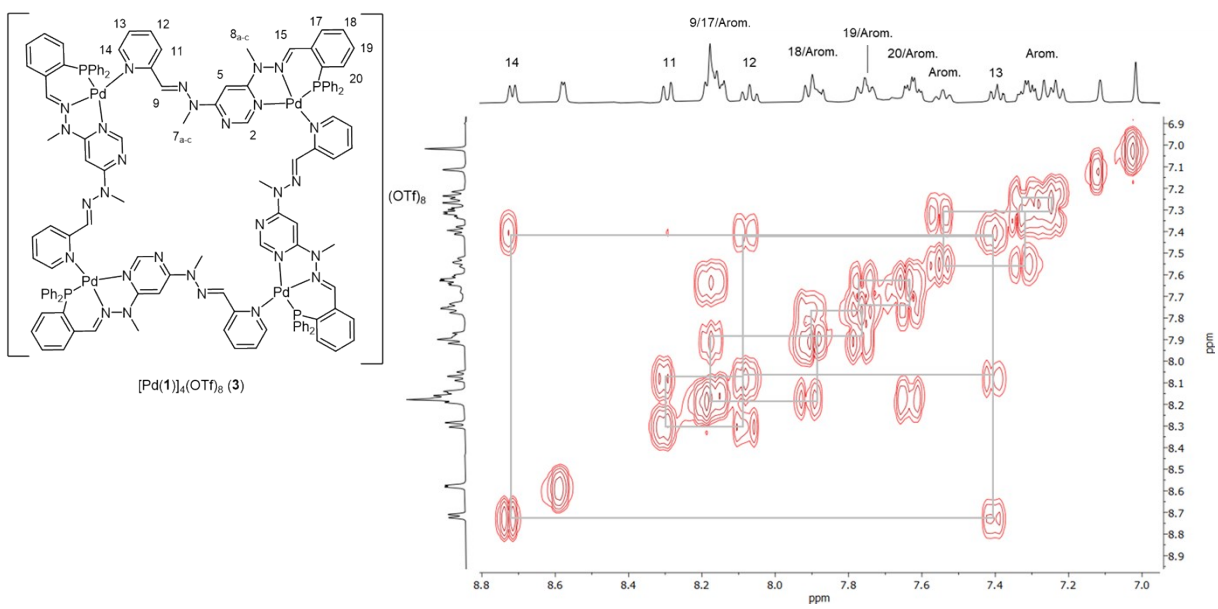


Figure S13. 1H - 1H COSY spectrum of **3** in CD_3CN at 25 °C.

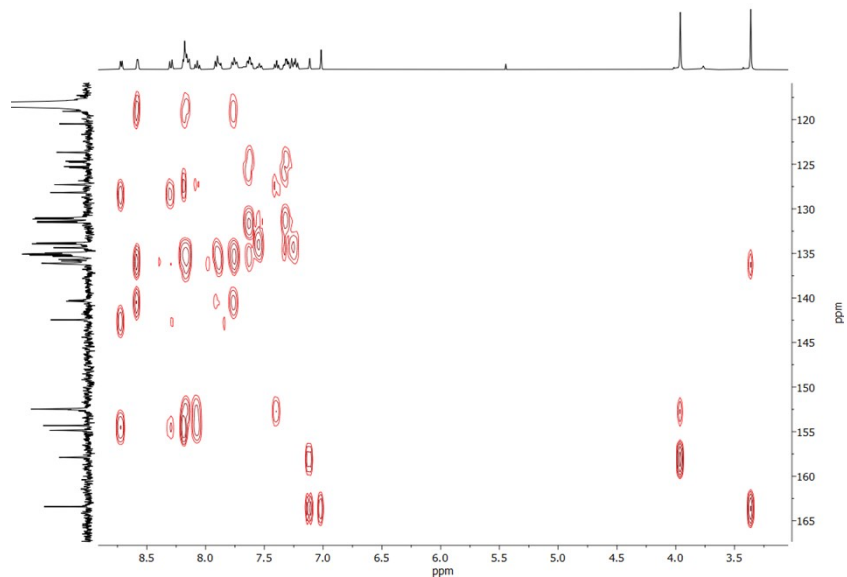


Figure S14. 1H - ^{13}C HMBC spectrum of **3** in CD_3CN at 25 °C.

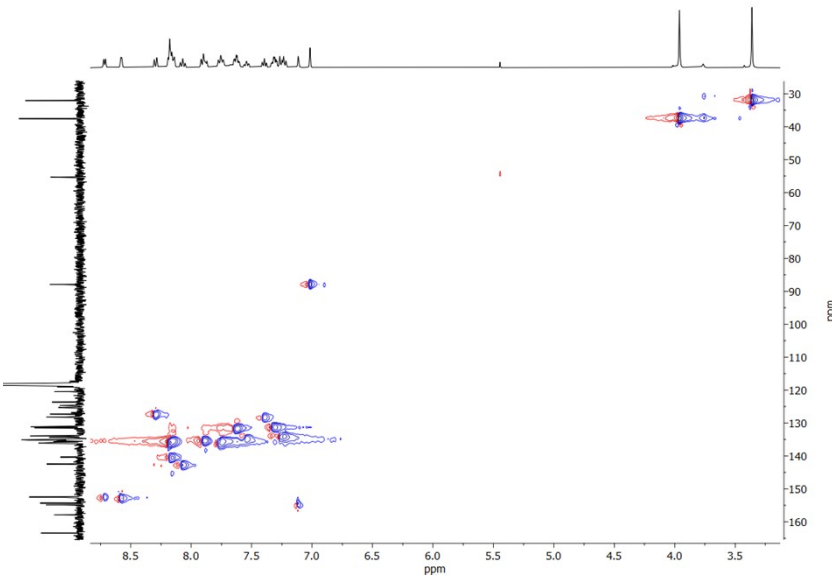


Figure S15. ^1H - ^{13}C HSQC spectrum of **3** in CD_3CN at 25°C .

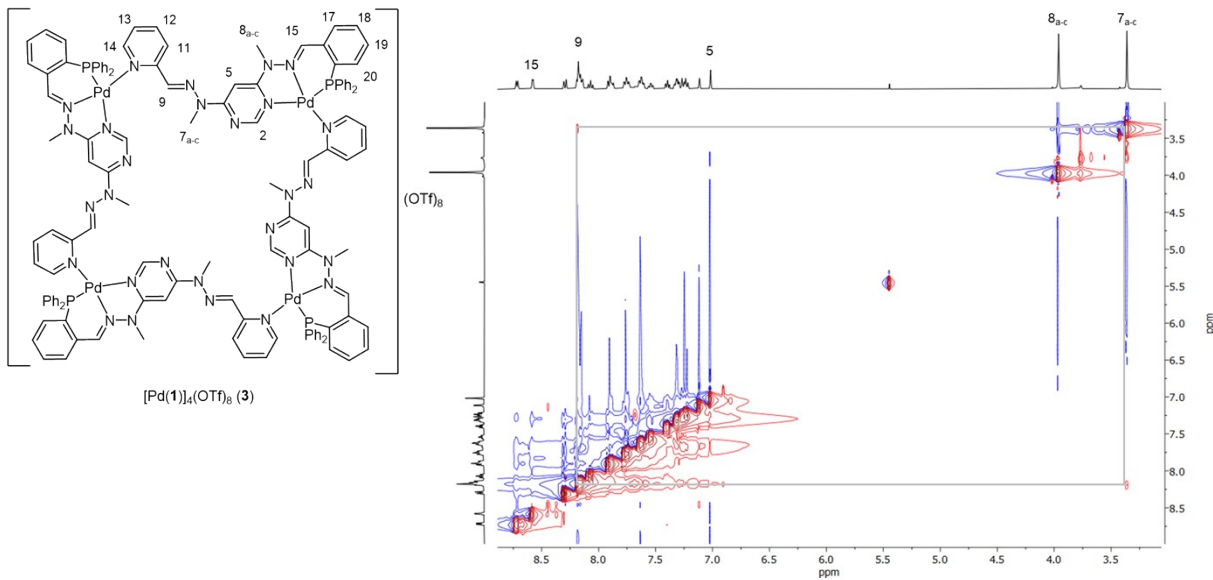


Figure S16. ^1H - ^1H NOESY spectrum of **3** in CD_3CN at 25°C .

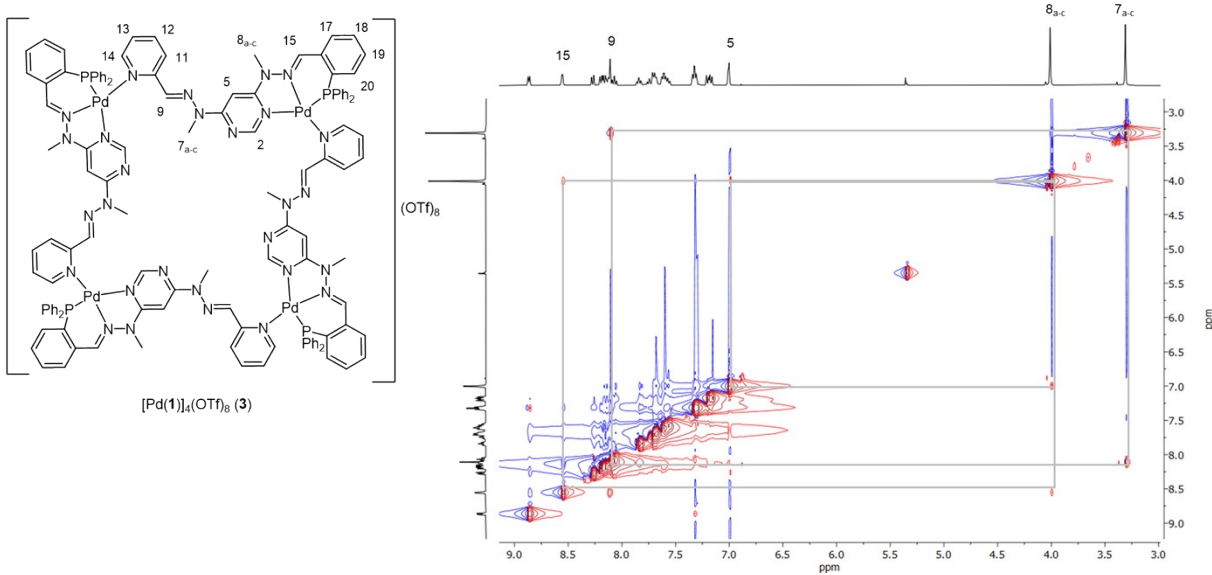


Figure S17. ¹H-¹H NOESY spectrum of **3** in CD₂Cl₂ at 25 °C.

3. NMR Spectra (¹H, ¹³C{¹H}, ¹⁹F{¹H}, ³¹P{¹H}, ¹H-¹H COSY, ¹H-¹³C HMBC, ¹H-¹³C HSQC) of **4**

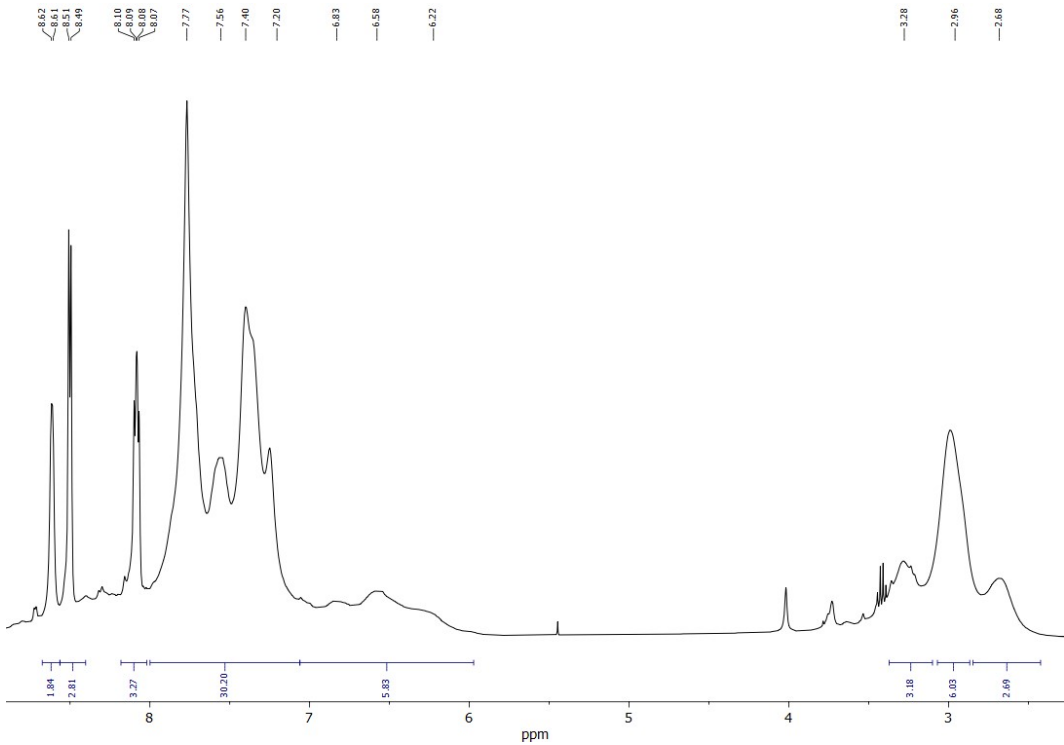


Figure S18. ¹H NMR spectrum of **4** in CD₃CN at 25 °C.

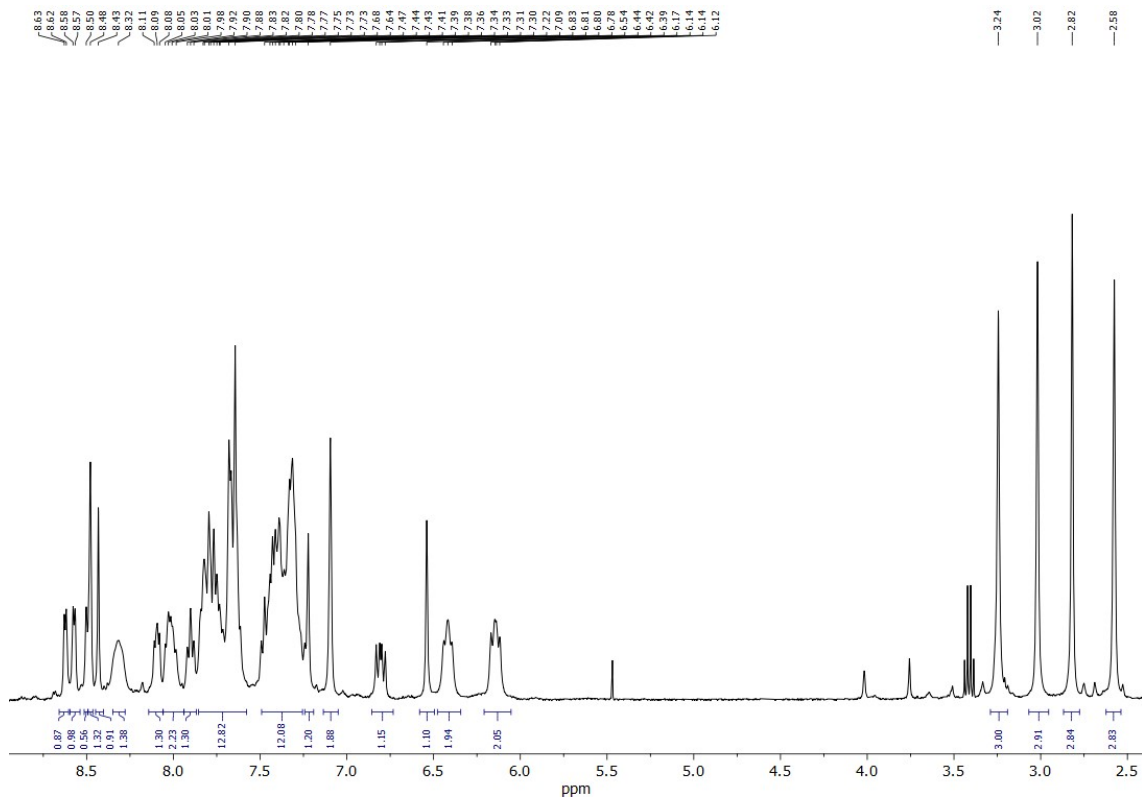


Figure S19. ^1H NMR spectrum of **4** in CD_3CN at -5°C .

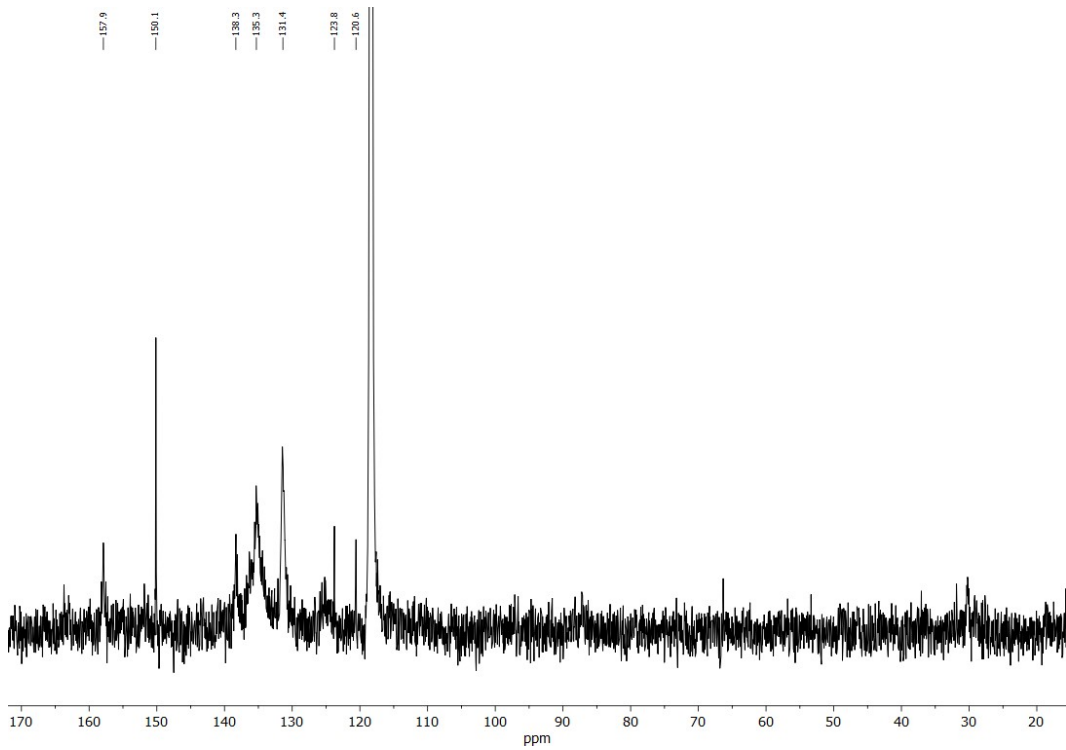


Figure S20. $^{13}\text{C}\{\text{H}\}$ NMR spectrum of **4** in CD_3CN at 25 °C.

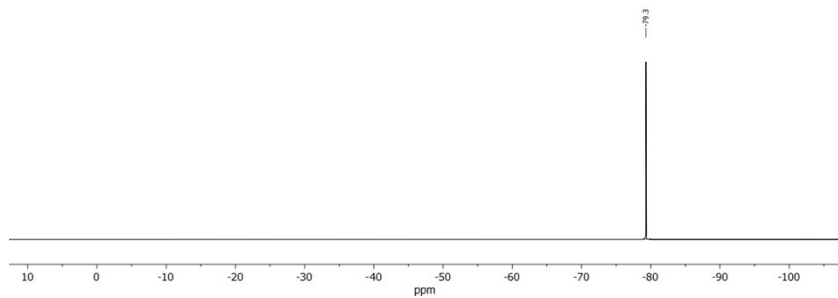


Figure S21. $^{19}\text{F}\{^1\text{H}\}$ NMR spectrum of **4** in CD_3CN at 25 °C.

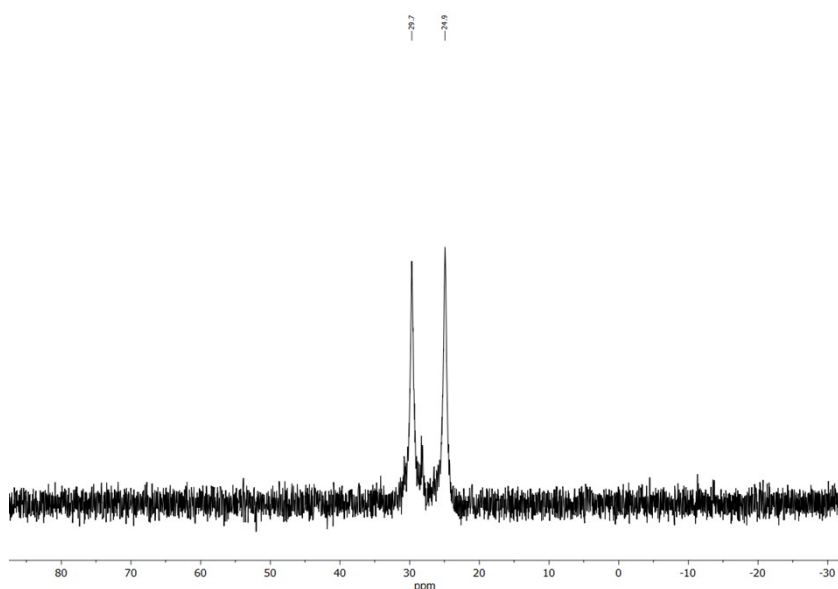


Figure S22. $^{31}\text{P}\{^1\text{H}\}$ NMR spectrum of **4** in CD_3CN at 25 °C.

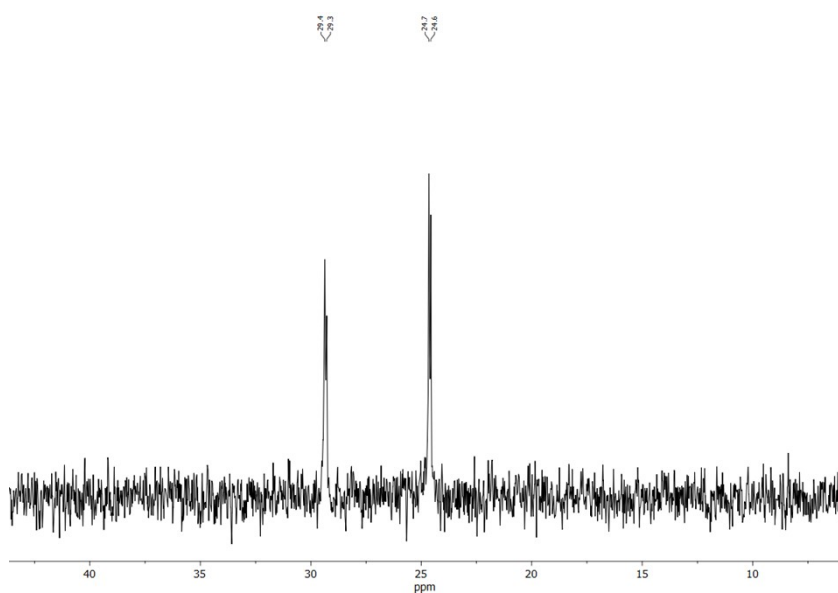


Figure S23. $^{31}\text{P}\{^1\text{H}\}$ NMR spectrum of **4** in CD_3CN at -5 °C.

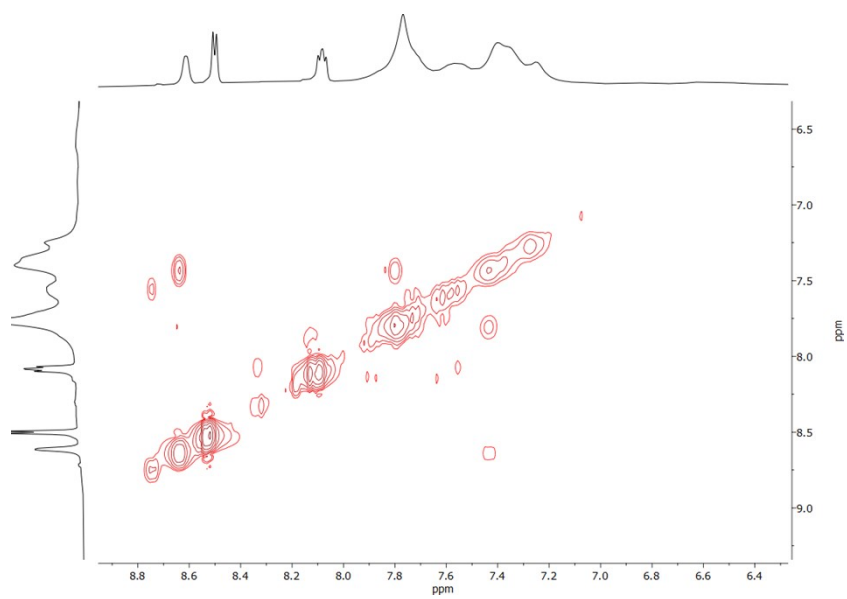


Figure S24. ^1H - ^1H COSY spectrum of of **4** in CD_3CN at 25 °C.

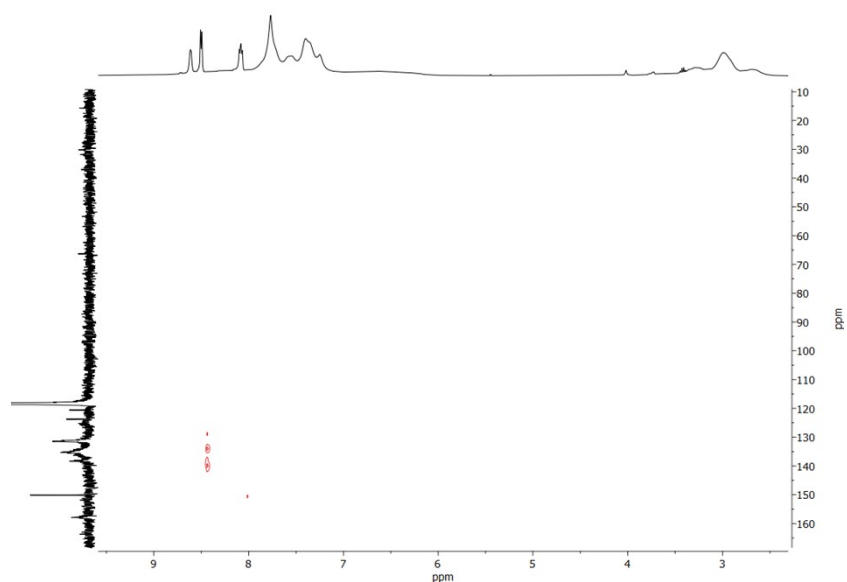


Figure S25. ^1H - ^{13}C HMBC spectrum of **4** in CD_3CN at 25 °C.

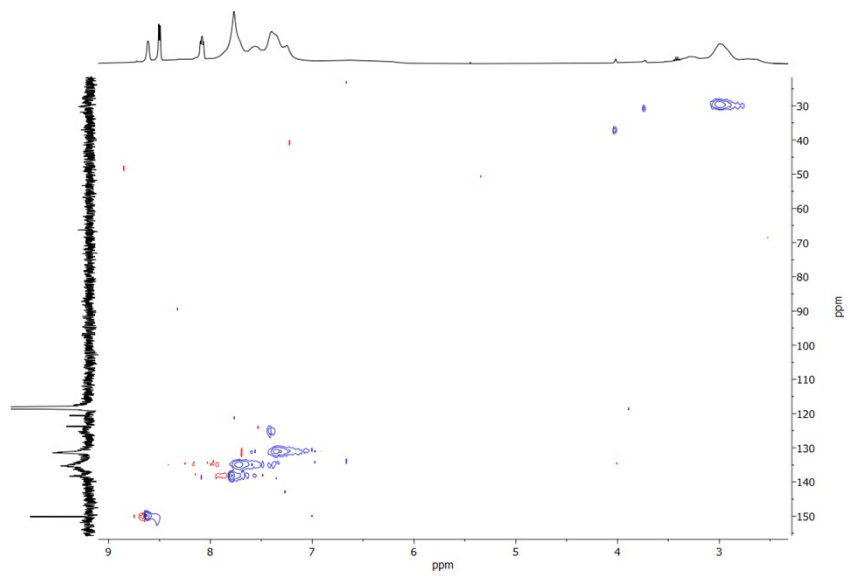


Figure S26. ¹H-¹³C HSQC spectrum of **4** in CD₃CN at 25 °C.

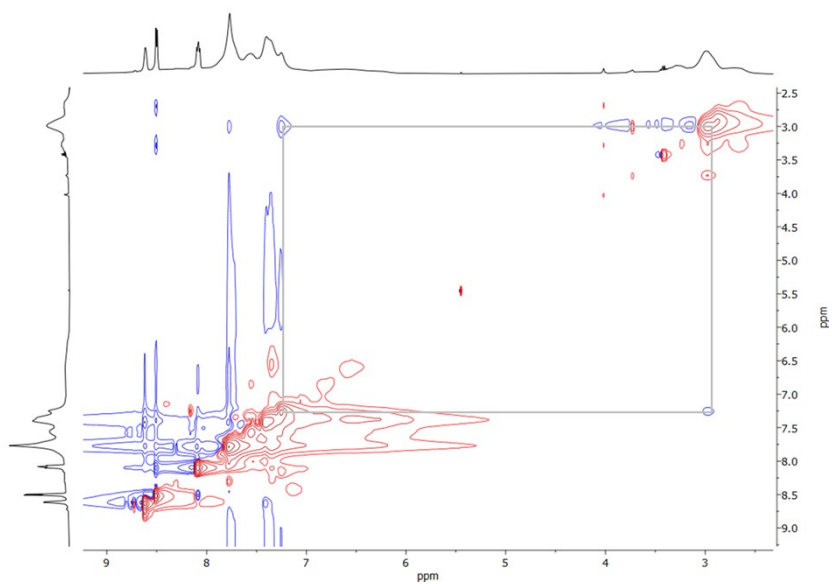


Figure S27. ¹H-¹H NOESY spectrum of **4** in CD₃CN at 25 °C.

4. NMR Spectra (^1H , $^{13}\text{C}\{^1\text{H}\}$, $^{19}\text{F}\{^1\text{H}\}$, $^{31}\text{P}\{^1\text{H}\}$, ^1H - ^1H COSY, ^1H - ^{13}C HMBC, ^1H - ^{13}C HSQC, ^1H - ^1H NOESY) of 5

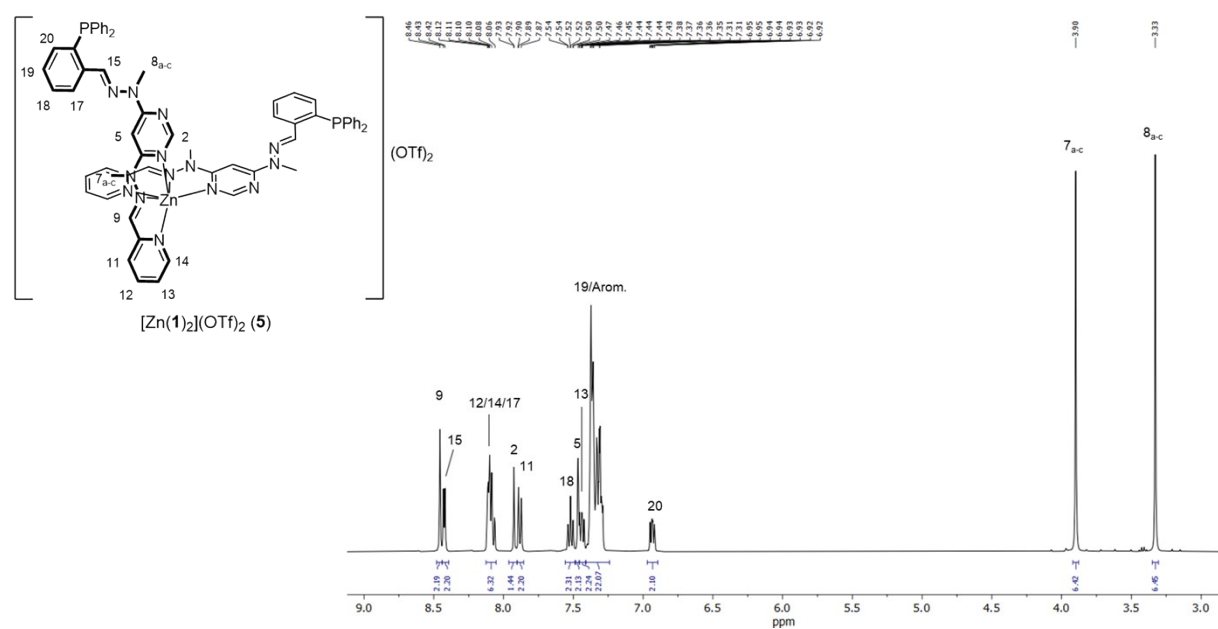


Figure S28. ^1H NMR spectrum of 5 in CD_3CN at 25 °C.

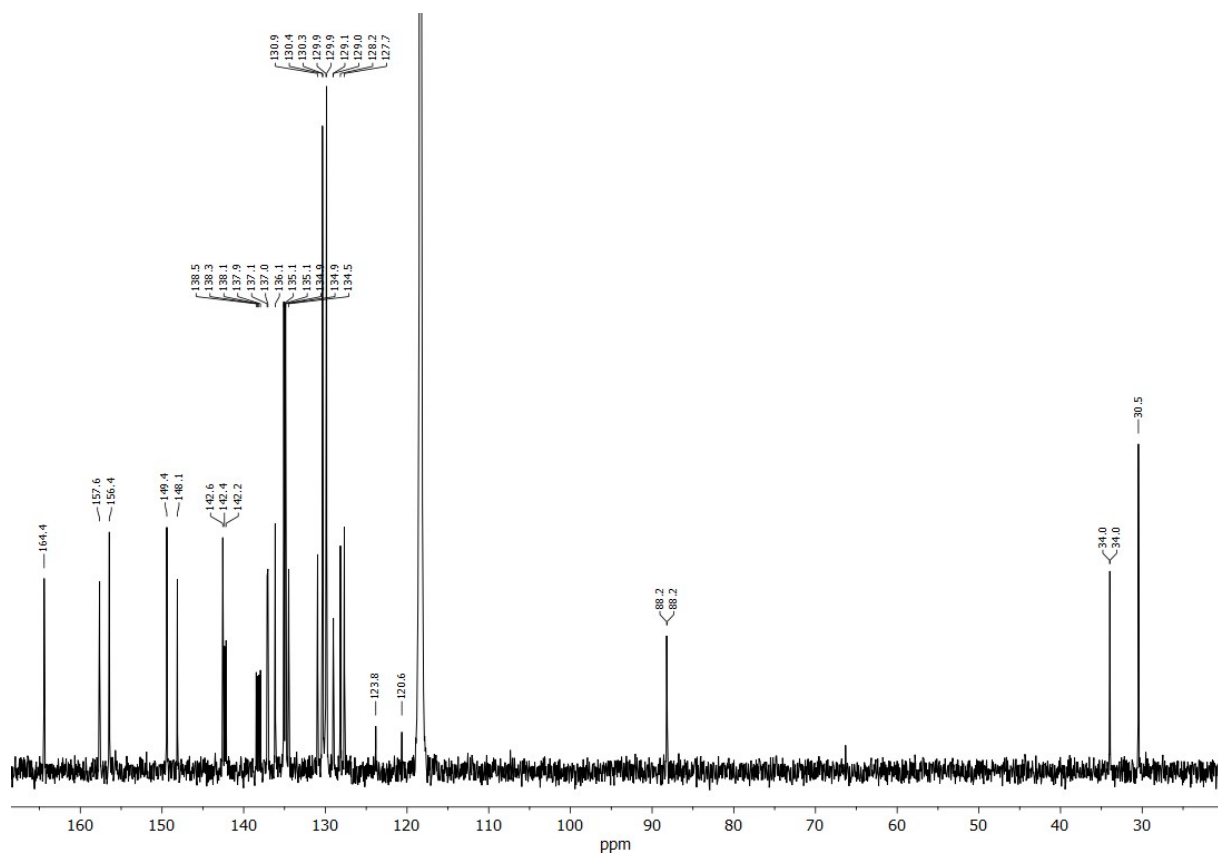


Figure S29. $^{13}\text{C}\{^1\text{H}\}$ NMR spectrum of 5 in CD_3CN at 25 °C.

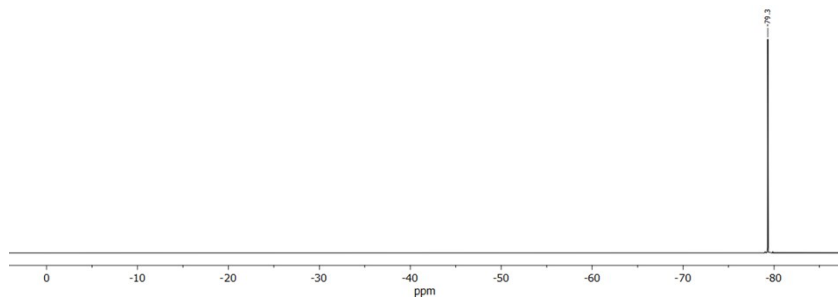


Figure S30. $^{19}\text{F}\{\text{H}\}$ NMR spectrum of **5** in CD_3CN at $25\text{ }^\circ\text{C}$.

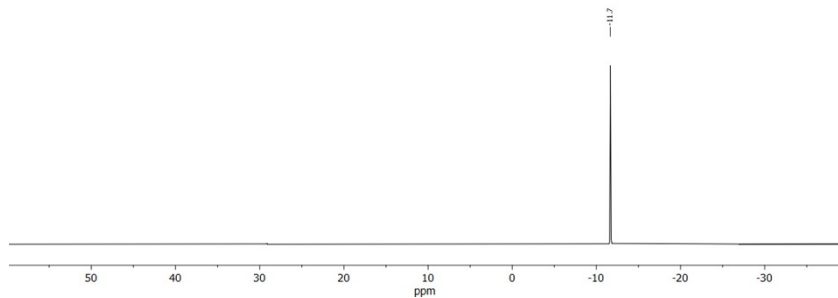


Figure S31. $^{31}\text{P}\{\text{H}\}$ NMR spectrum of **5** in CD_3CN at $25\text{ }^\circ\text{C}$.

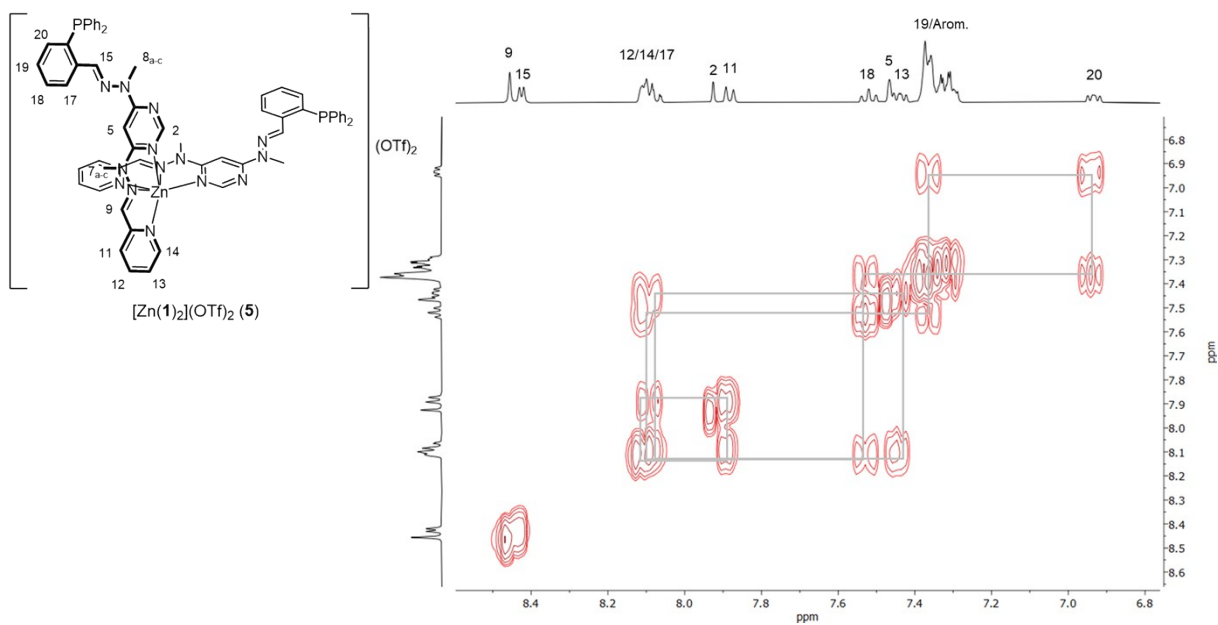


Figure S32. ^1H - ^1H COSY spectrum of **5** in CD_3CN at $25\text{ }^\circ\text{C}$.

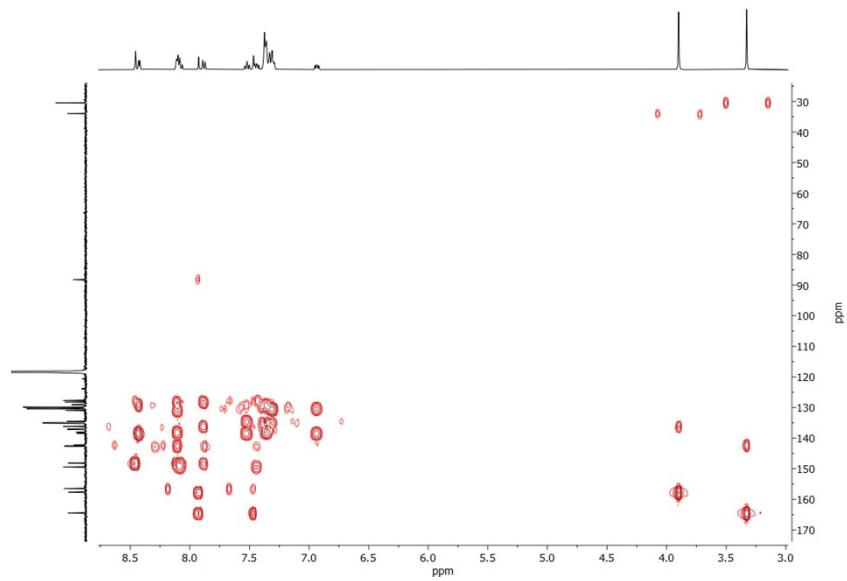


Figure S33. ^1H - ^{13}C HMBC spectrum of **5** in CD_3CN at 25 °C.

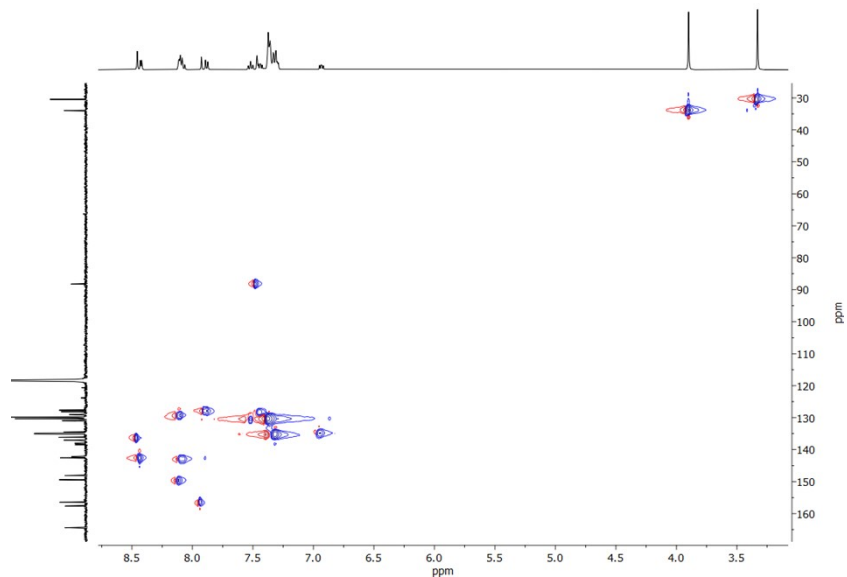


Figure S34. ^1H - ^{13}C HSQC spectrum of **5** in CD_3CN at 25 °C.

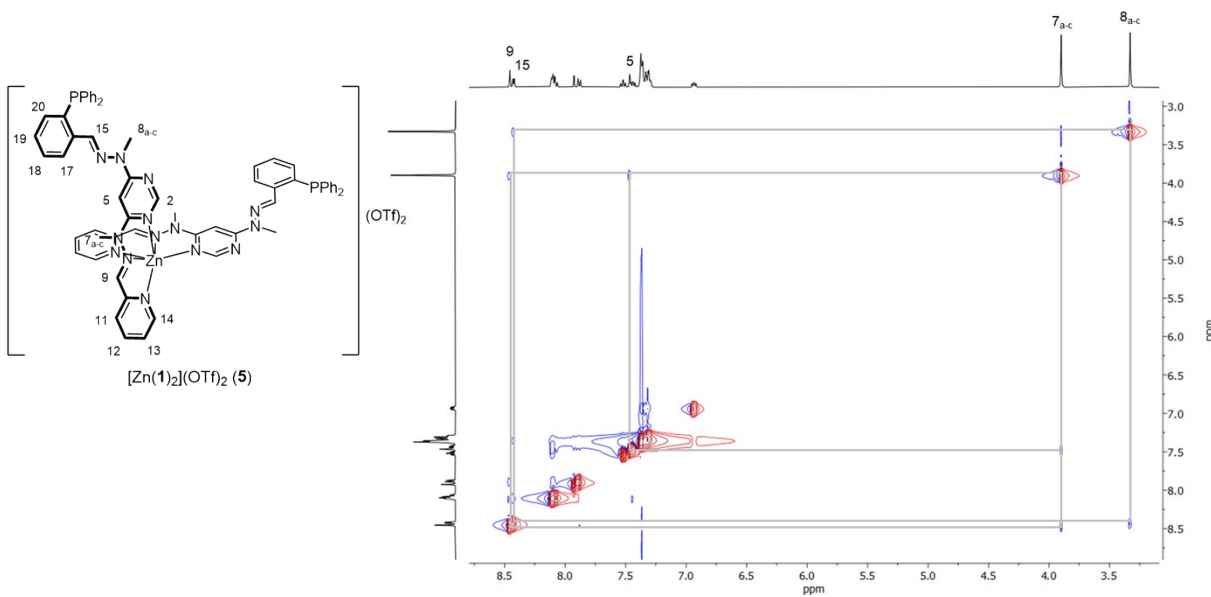


Figure S35. ^1H - ^1H NOESY spectrum of **5** in CD_3CN at 25 °C.

5. NMR Spectra (^1H , $^{13}\text{C}\{^1\text{H}\}$, $^{19}\text{F}\{^1\text{H}\}$, $^{31}\text{P}\{^1\text{H}\}$, ^1H - ^1H COSY, ^1H - ^{13}C HMBC, ^1H - ^{13}C HSQC, ^1H - ^1H NOESY) of **6**

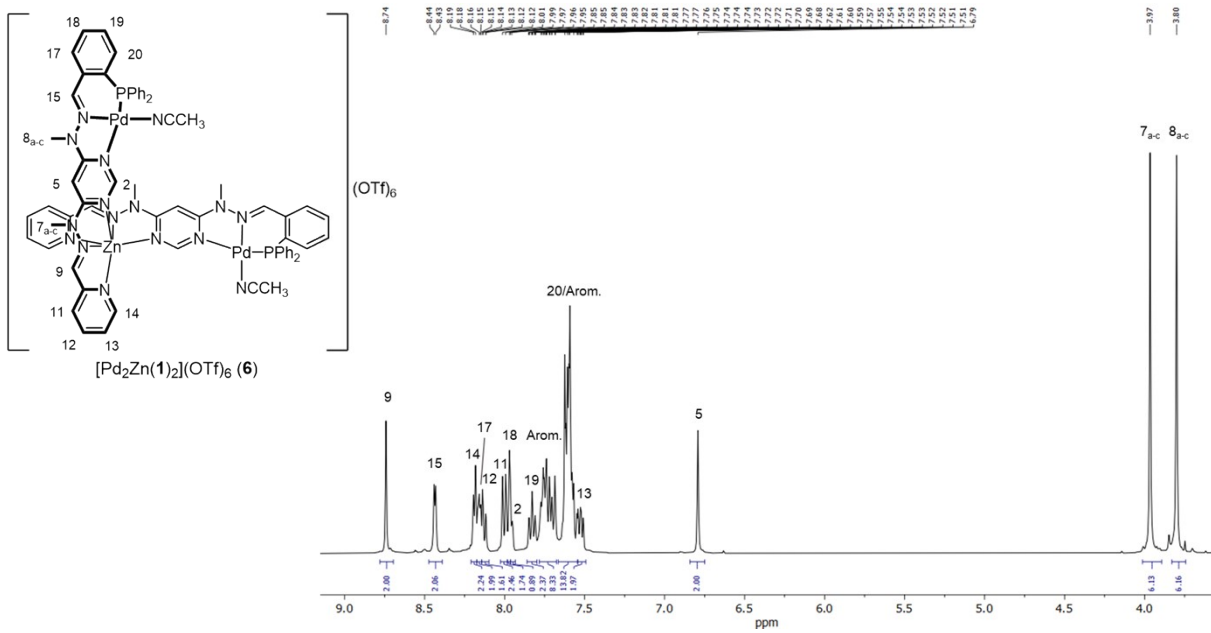


Figure S36. ^1H NMR spectrum of **6** in CD_3CN at 25 °C.

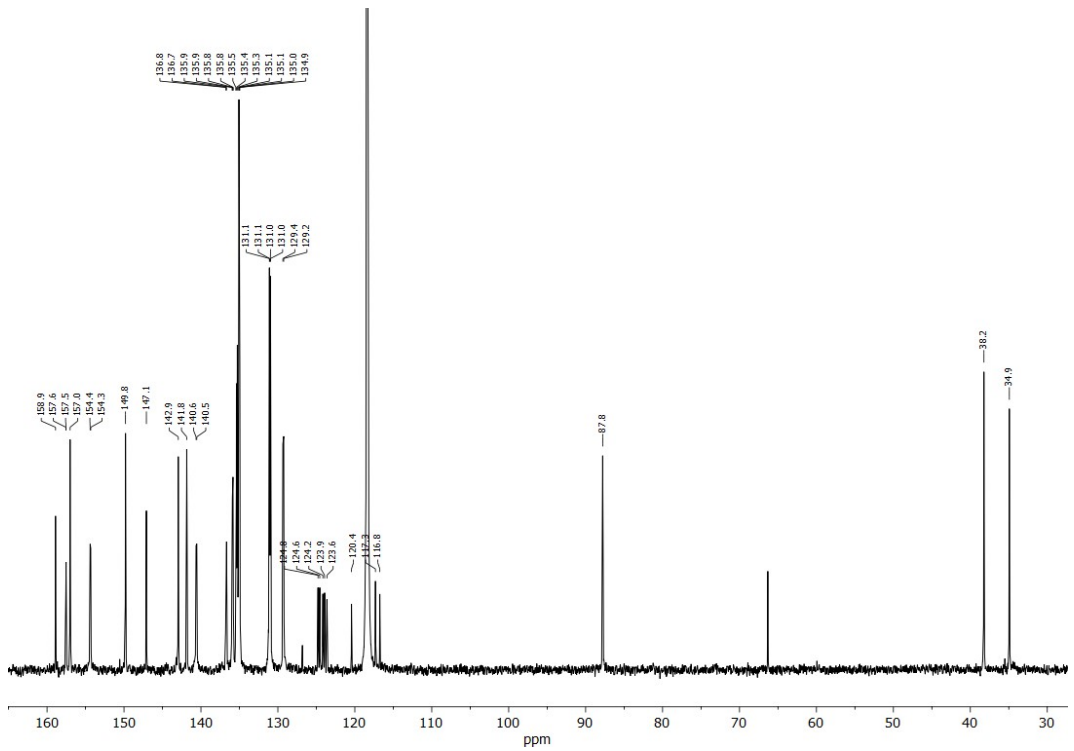


Figure S37. $^{13}\text{C}\{^1\text{H}\}$ NMR spectrum of **6** in CD_3CN at $25\text{ }^\circ\text{C}$.

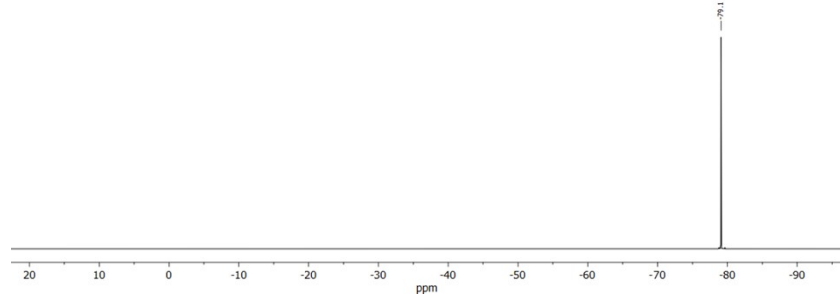


Figure S38. $^{19}\text{F}\{^1\text{H}\}$ NMR spectrum of **6** in CD_3CN at $25\text{ }^\circ\text{C}$.

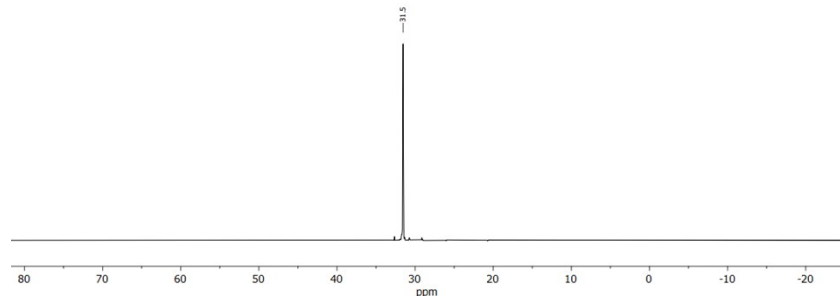


Figure S39. $^{31}\text{P}\{^1\text{H}\}$ NMR spectrum of **6** in CD_3CN at $25\text{ }^\circ\text{C}$.

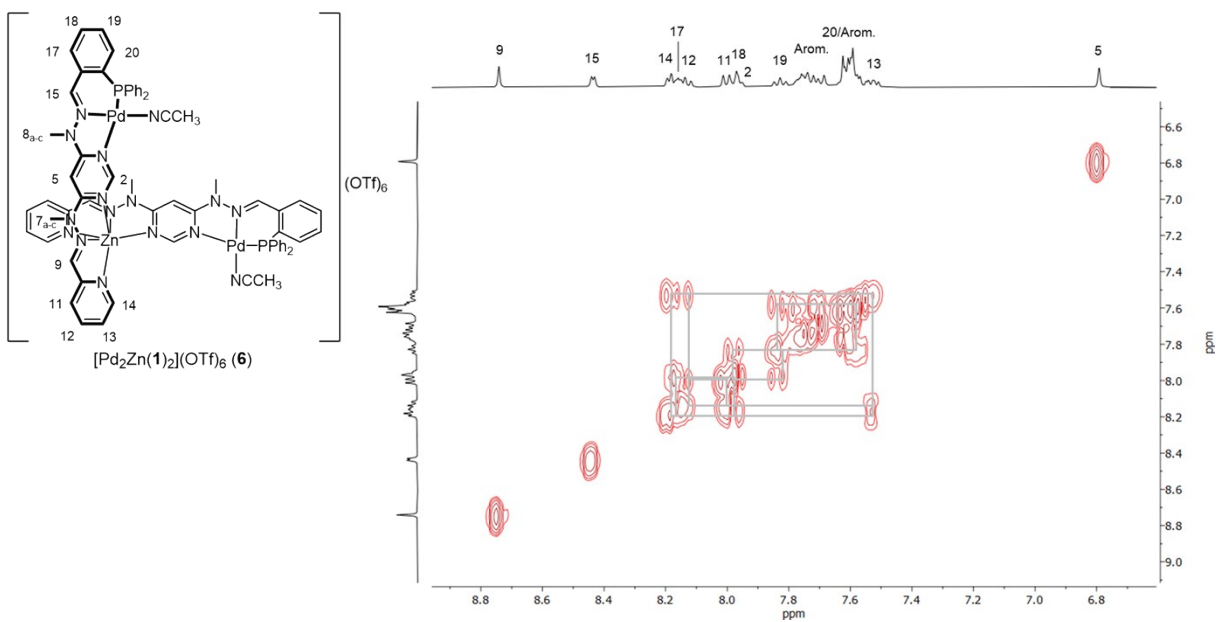


Figure S40. 1H - 1H COSY spectrum of **6** in CD_3CN at 25 °C.

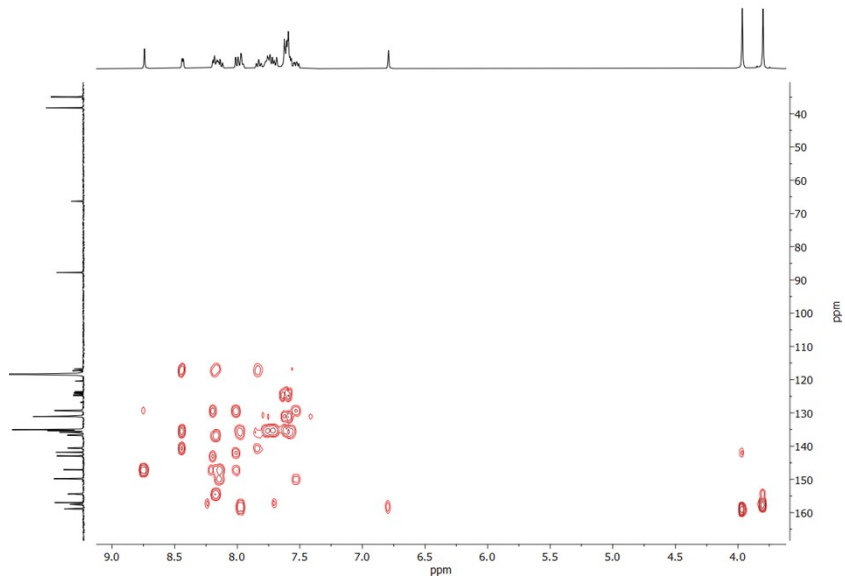


Figure S41. 1H - ^{13}C HMBC spectrum of **6** in CD_3CN at 25 °C.

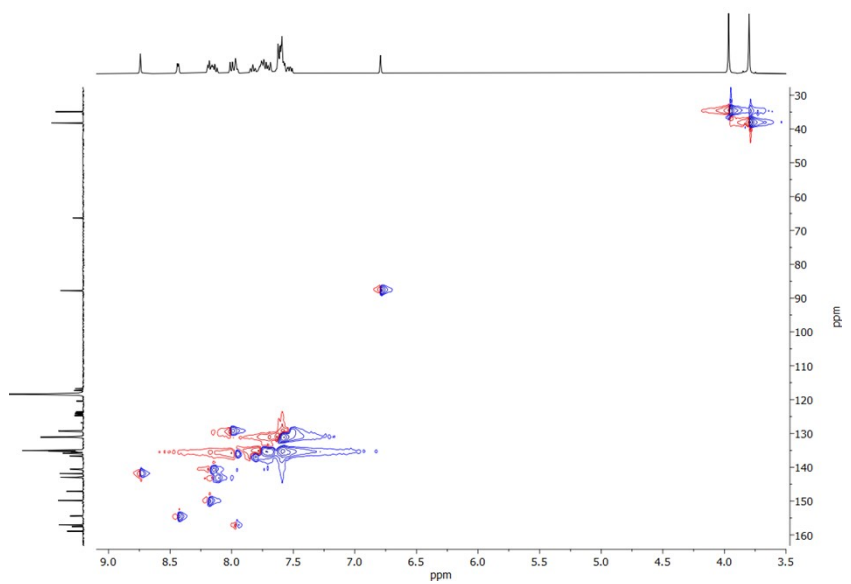


Figure S42. ^1H - ^{13}C HSQC spectrum of **6** in CD_3CN at 25°C .

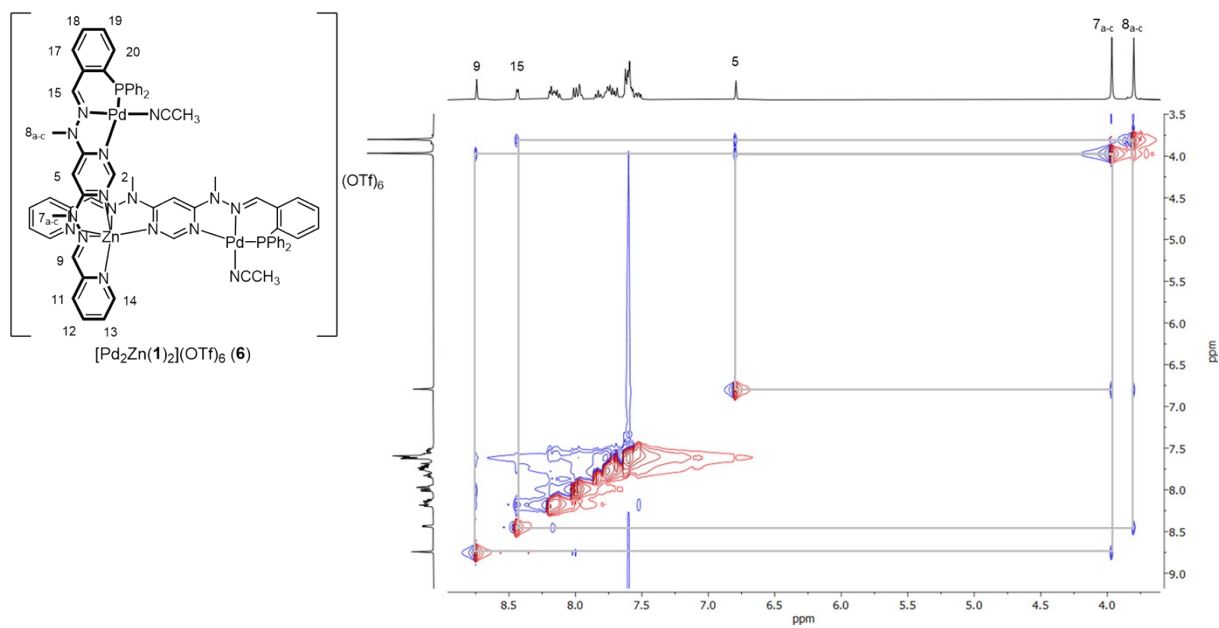


Figure S43. ^1H - ^1H NOESY spectrum of **6** in CD_3CN at 25°C .

6. NMR Spectra (^1H , $^{13}\text{C}\{^1\text{H}\}$, $^{19}\text{F}\{^1\text{H}\}$, $^{31}\text{P}\{^1\text{H}\}$, ^1H - ^1H COSY, ^1H - ^{13}C HMBC, ^1H - ^{13}C HSQC, ^1H - ^1H NOESY) of 7

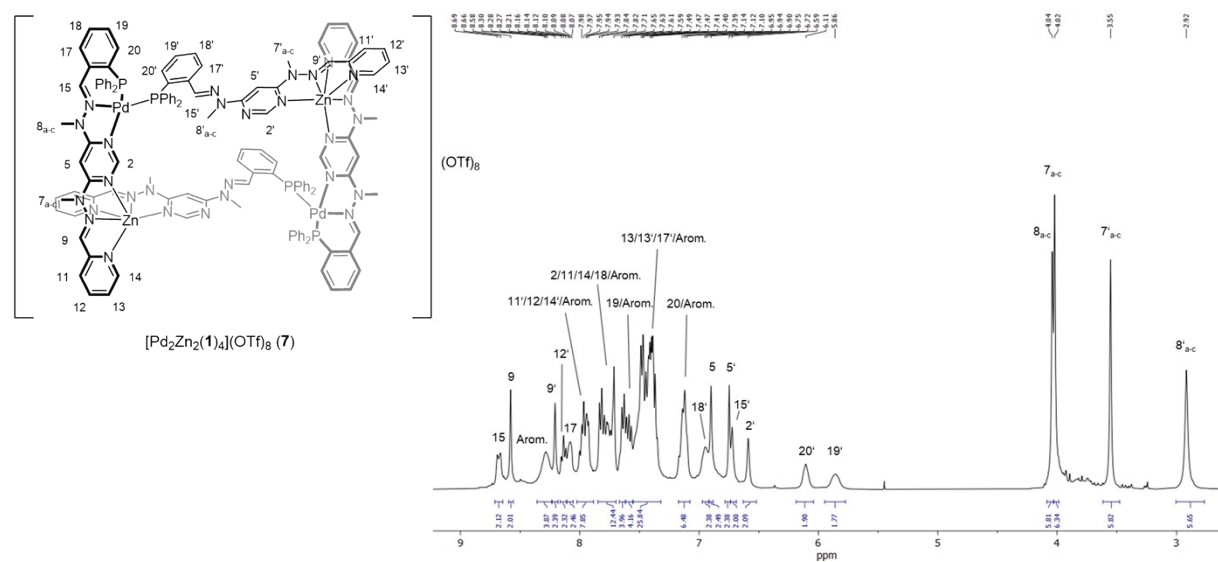


Figure S44. ^1H NMR spectrum of 7 in CD_3CN at 25 °C.

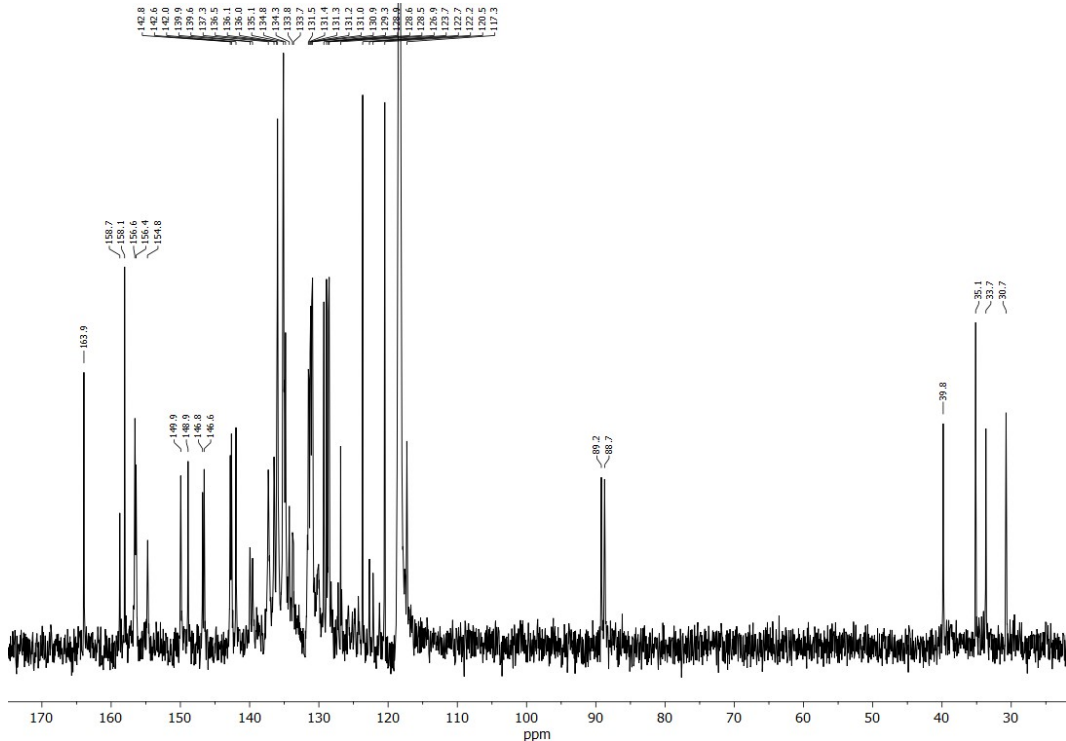


Figure S45. $^{13}\text{C}\{^1\text{H}\}$ NMR spectrum of 7 in CD_3CN at 25 °C.

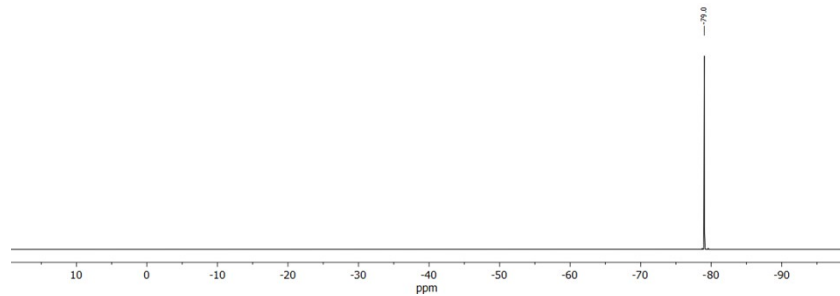


Figure S46. $^{19}\text{F}\{^1\text{H}\}$ NMR spectrum of **7** in CD_3CN at 25 °C.

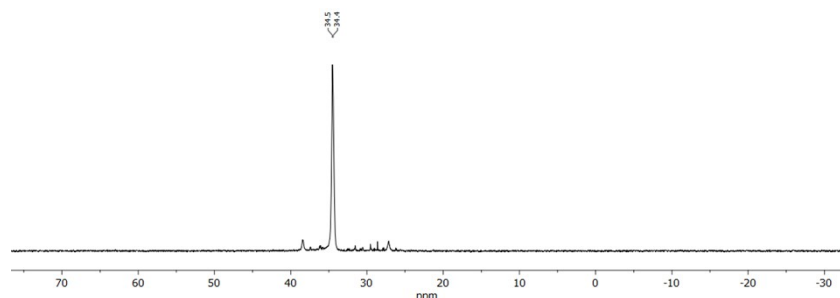


Figure S47. $^{31}\text{P}\{^1\text{H}\}$ NMR spectrum of **7** in CD_3CN at 25 °C.

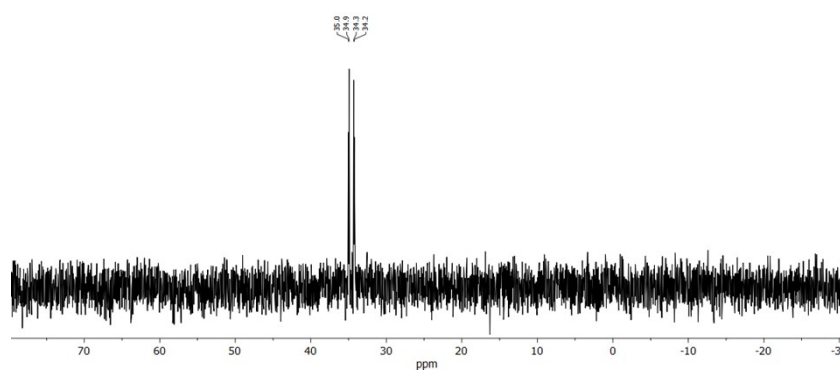


Figure S48. $^{31}\text{P}\{^1\text{H}\}$ NMR spectrum of **7** in CD_3CN at -5 °C.

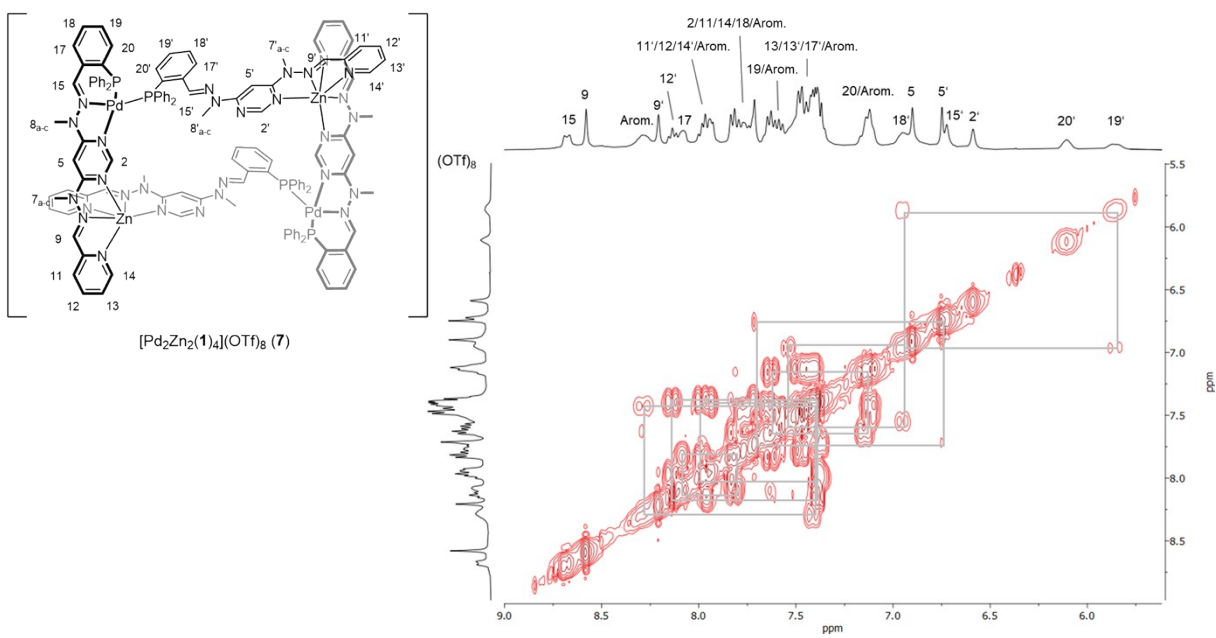


Figure S49. ^1H - ^1H COSY spectrum of **7** in CD_3CN at 25 °C.

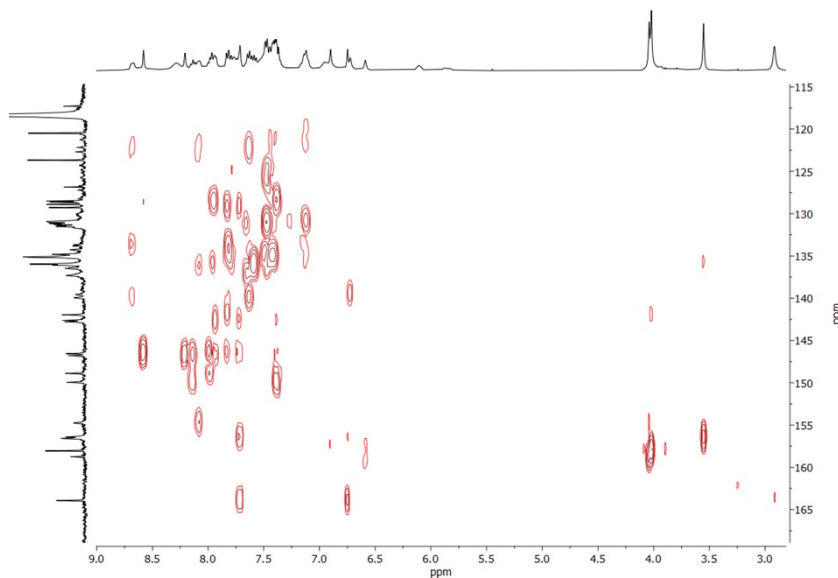


Figure S50. ^1H - ^{13}C HMBC spectrum of **7** in CD_3CN at 25 °C.

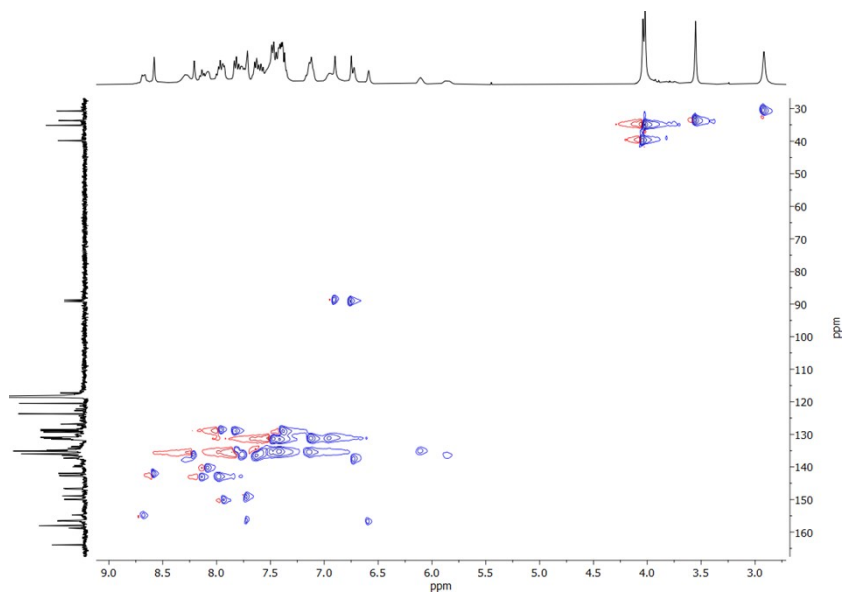


Figure S51. ^1H - ^{13}C HSQC spectrum of **7** in CD_3CN at 25°C .

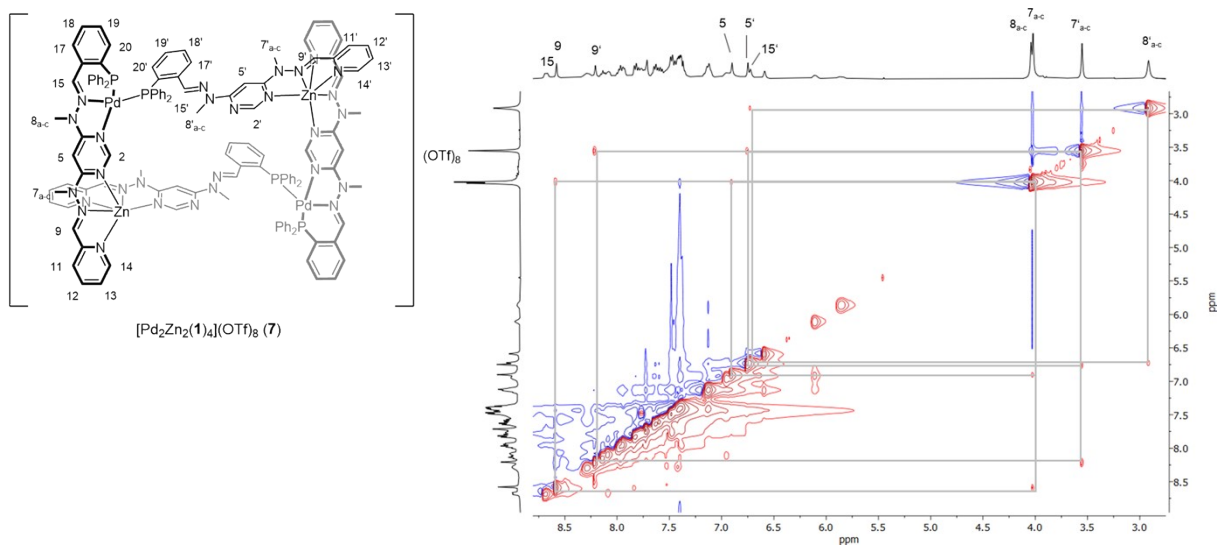


Figure S52. ^1H - ^1H NOESY spectrum of **7** in CD_3CN at 25°C .

7. VT NMR Spectra (^1H , $^{31}\text{P}\{^1\text{H}\}$) of **4** and **7**

VT ^1H NMR (400 MHz, CD_3CN) of **4**

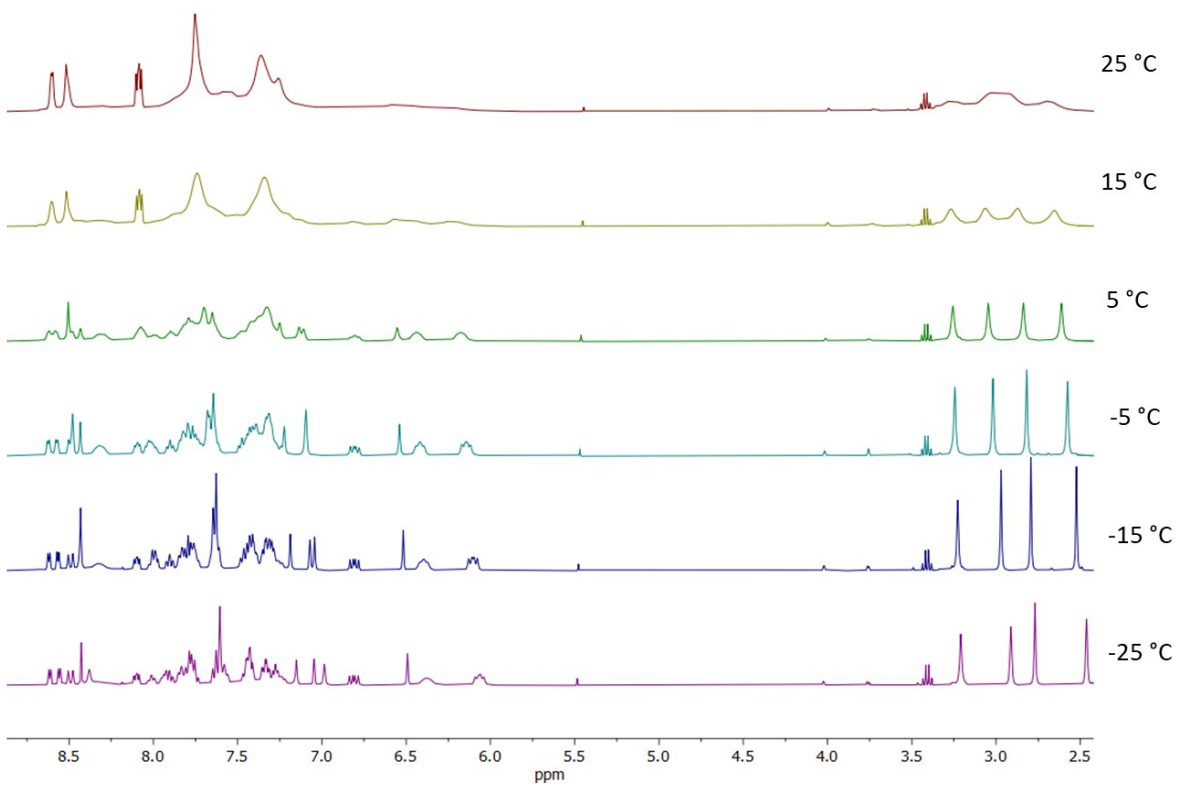


Figure S53. VT ^1H NMR spectra of **4** in CD_3CN from 25 °C to -25 °C.

VT ^1H NMR (400 MHz, CD_3CN) of **4**

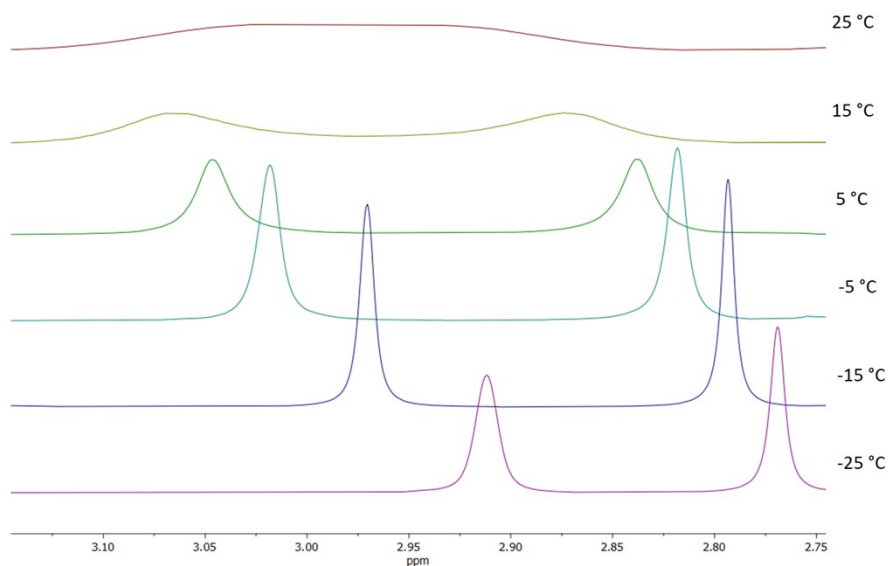


Figure S54. VT ^1H NMR spectra of **4** (signal at 3.00 ppm at 25 °C) in CD_3CN from 25 °C to -25 °C.

VT ^1H NMR (400 MHz, CD_3CN) of 4

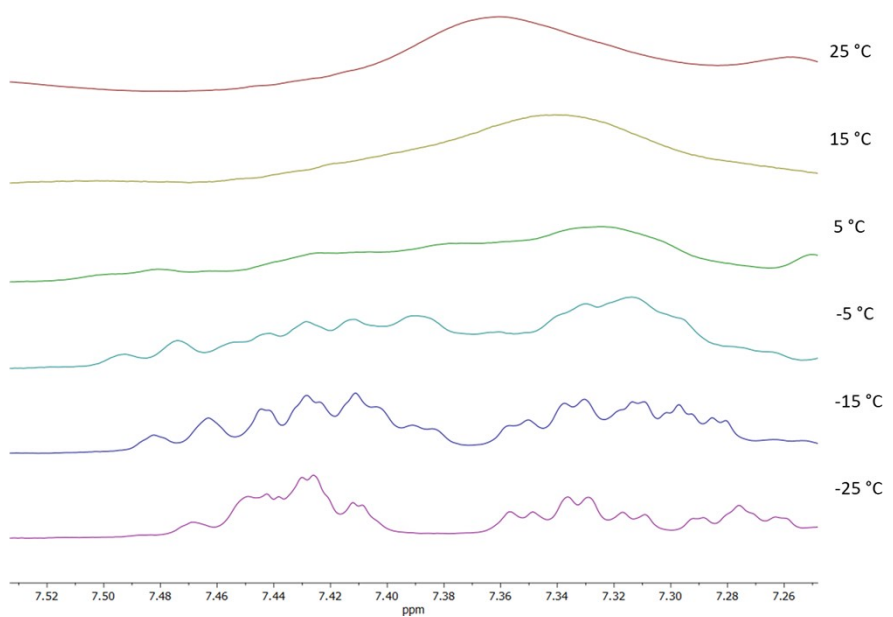


Figure S55. VT ^1H NMR spectra of 4 (signal at 7.36 ppm 25 °C) in CD_3CN from 25 °C to -25 °C.

VT ^1H NMR (400 MHz, CD_3CN) of 4

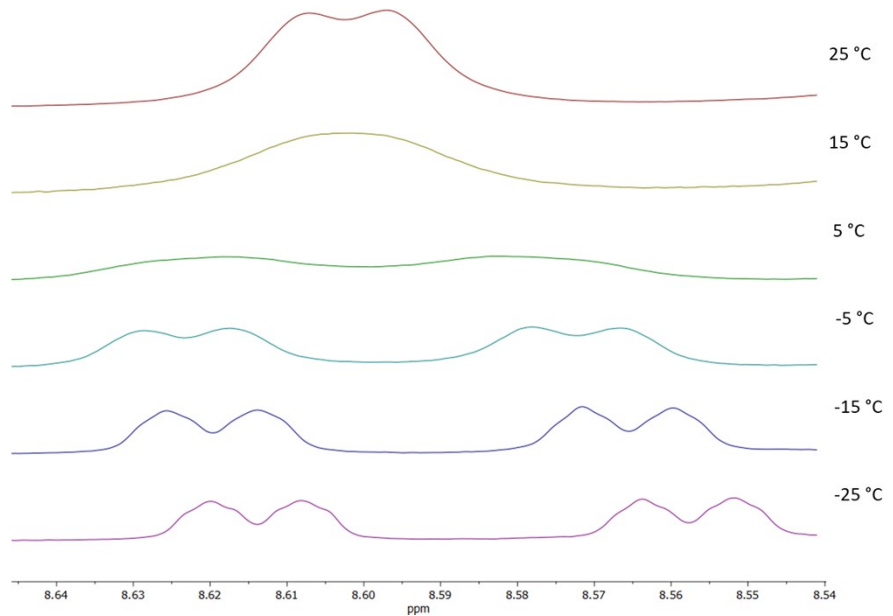


Figure S56. VT ^1H NMR spectra of 4 (signal at 8.60 ppm at 25 °C) in CD_3CN from 25 °C to -25 °C.

VT $^{31}\text{P}\{\text{H}\}$ NMR (162 MHz, CD_3CN) of 4

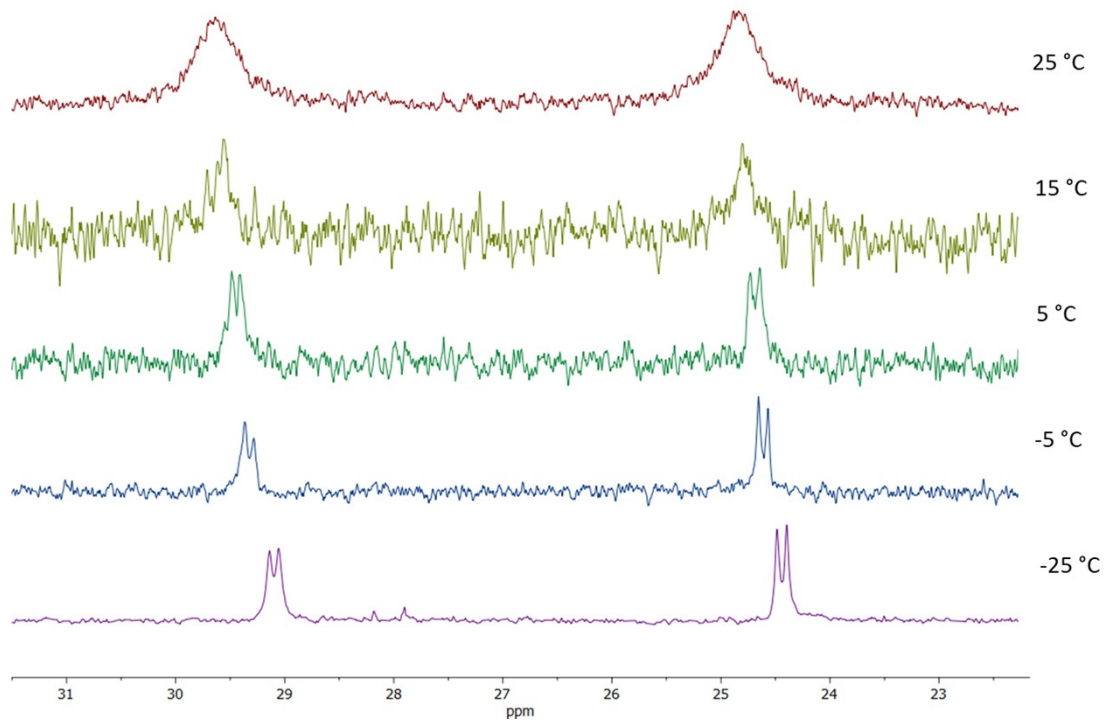


Figure S57. VT $^{31}\text{P}\{\text{H}\}$ NMR spectra of **4** in CD_3CN from 25°C to -25°C .

VT ^1H NMR (400 MHz, CD_3CN) of 7

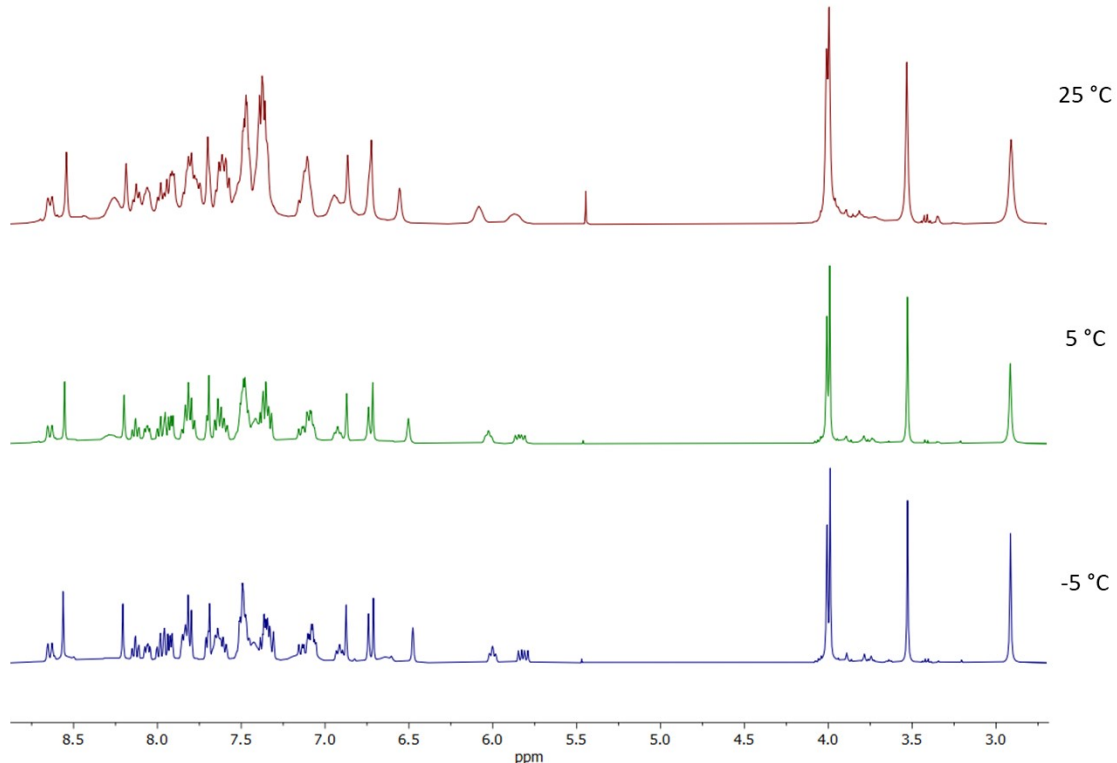


Figure S58. VT ^1H NMR spectra of **7** in CD_3CN from 25°C to -5°C .

VT $^{31}\text{P}\{\text{H}\}$ NMR (162 MHz, CD_3CN) of 7

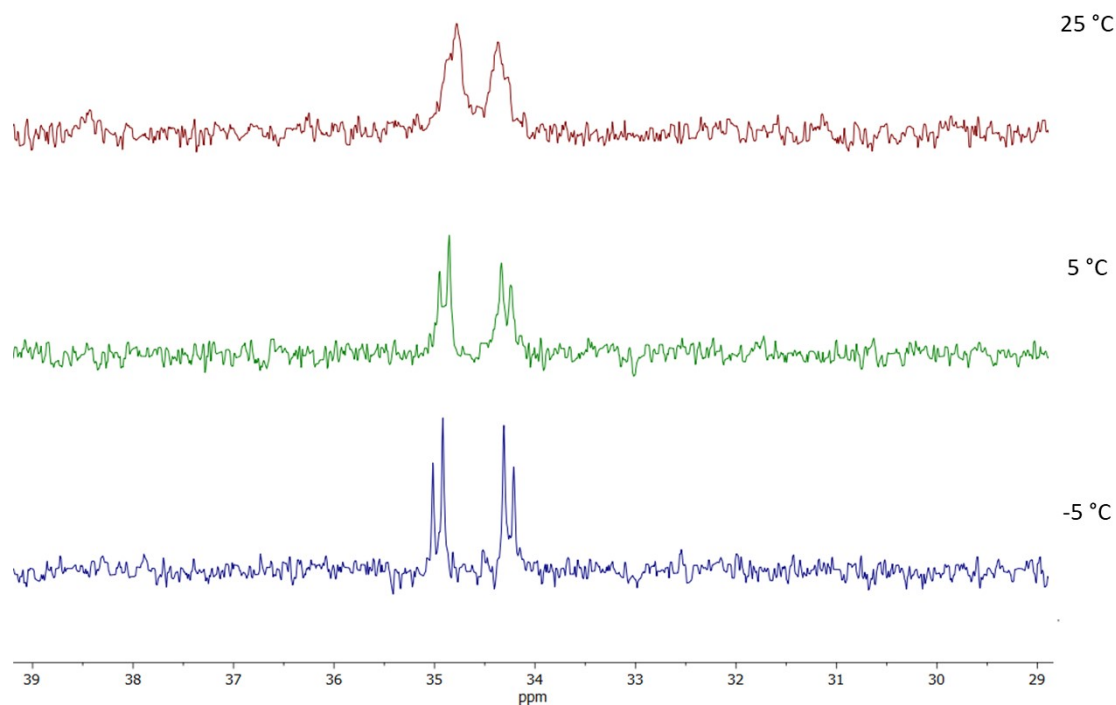
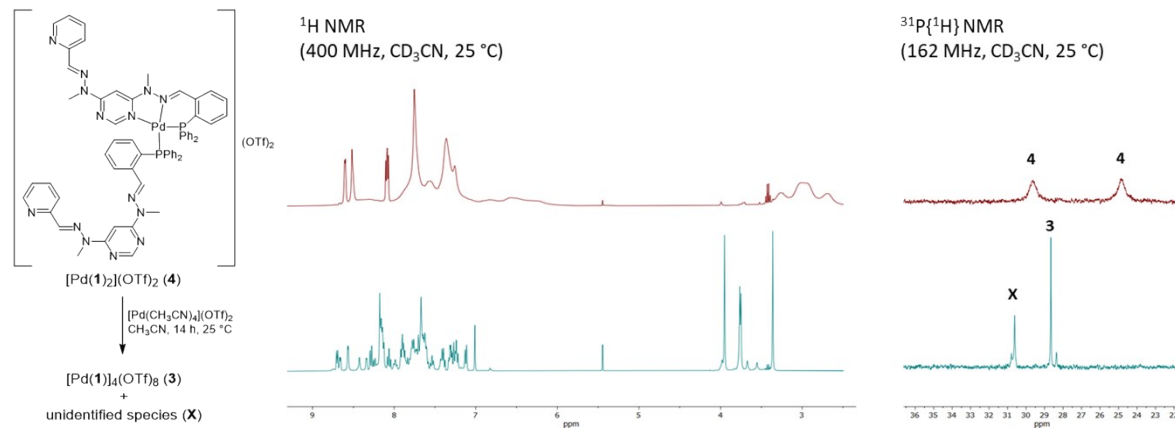


Figure S59. VT $^{31}\text{P}\{\text{H}\}$ NMR spectra of 7 in CD_3CN from 25 °C to -5 °C.

8. Reaction NMR Spectra



Scheme S1. ^1H and $^{31}\text{P}\{\text{H}\}$ NMR spectra of the reaction mixture of complex 4 with $[\text{Pd}(\text{CH}_3\text{CN})_4](\text{OTf})_2$ showing the formation of 3 and an unidentified species (X).

Reactions to form 7

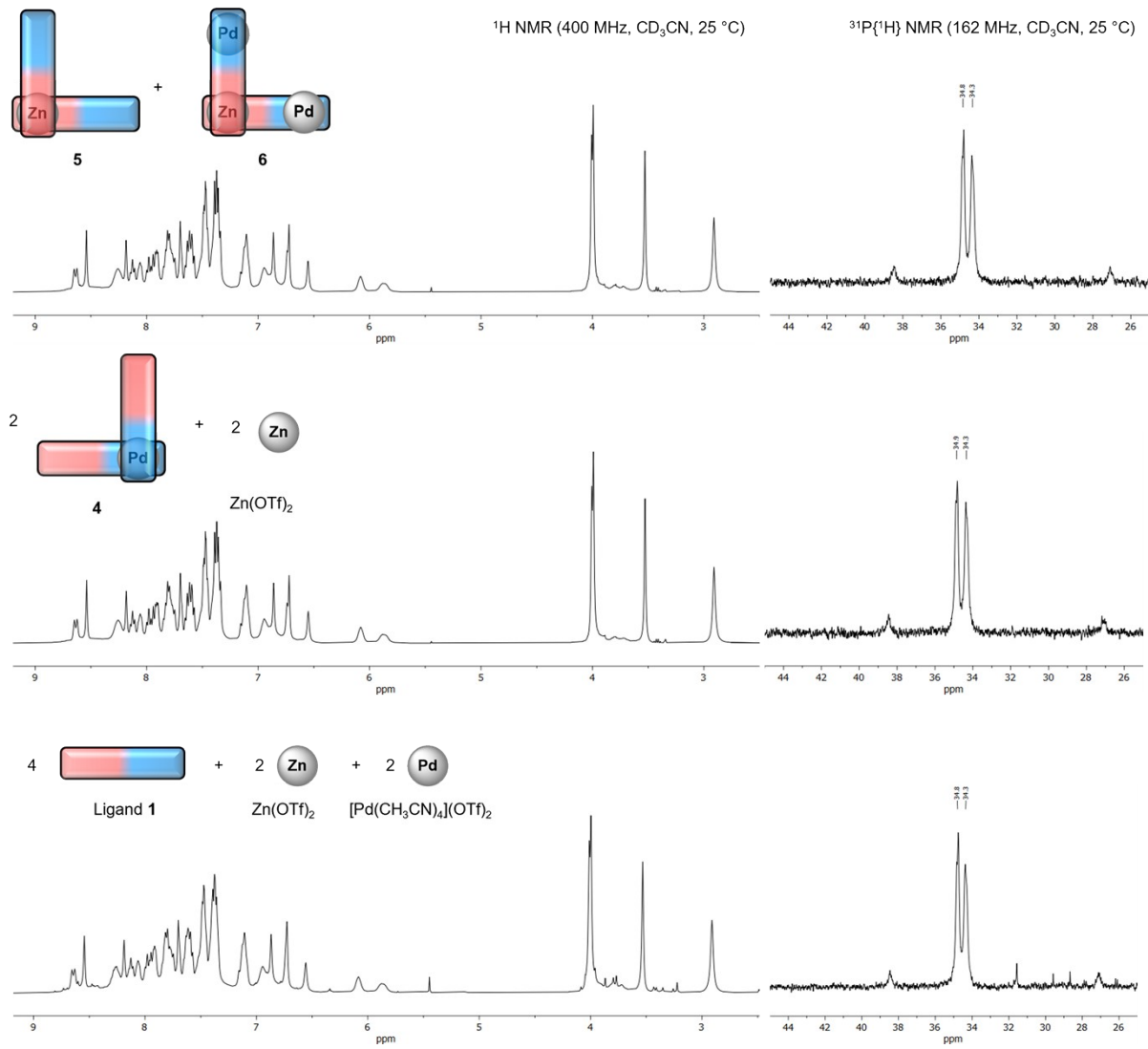
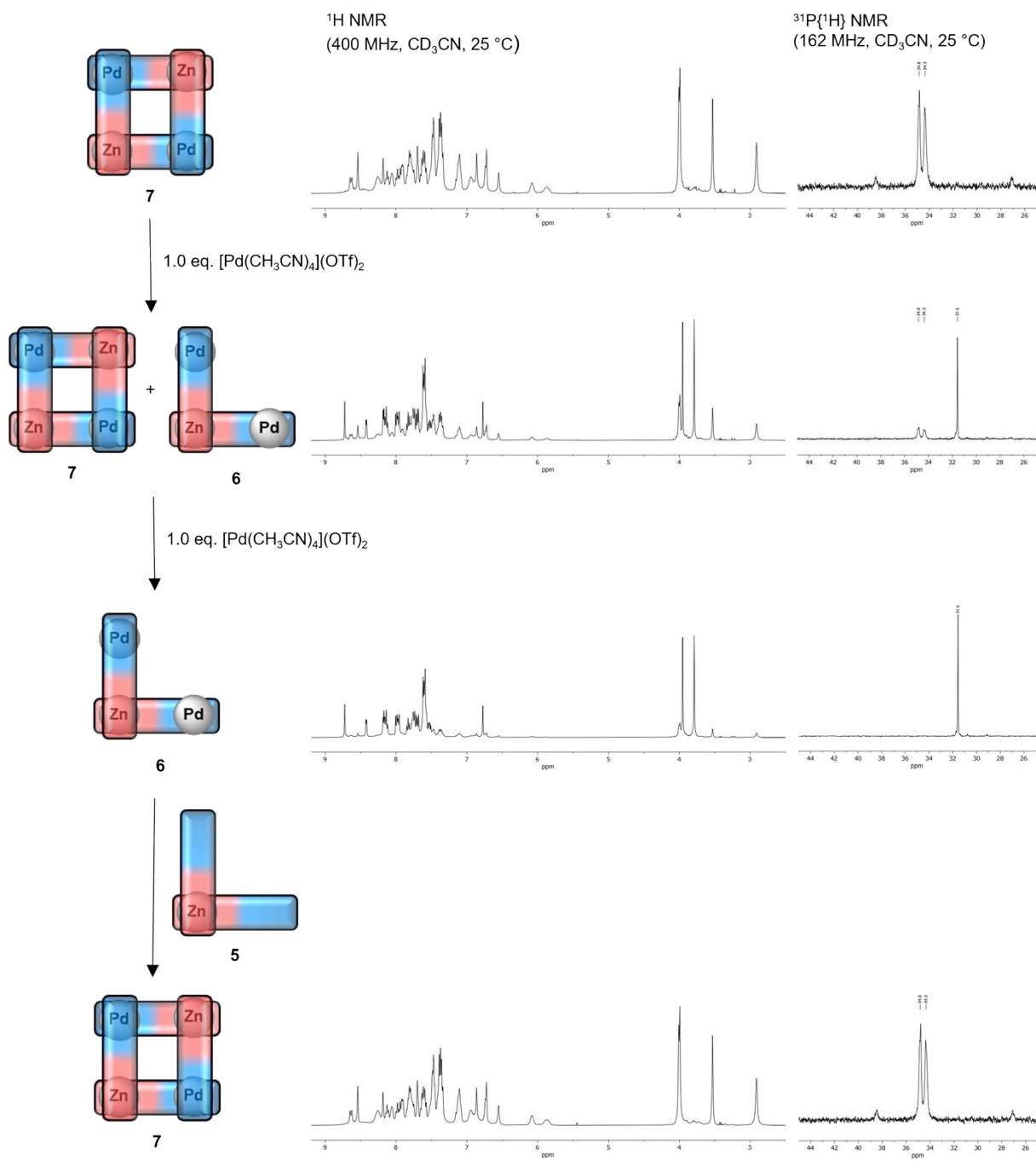


Figure S60. ¹H and ³¹P{¹H} NMR spectra of the formation of **7** based on different building blocks.

Disassembly and reassembly of 7



Scheme S2. ¹H and ³¹P{¹H} NMR spectra of the disassembly and reassembly of 7.

9. ^1H DOSY NMR Spectra of Complexes 2–7

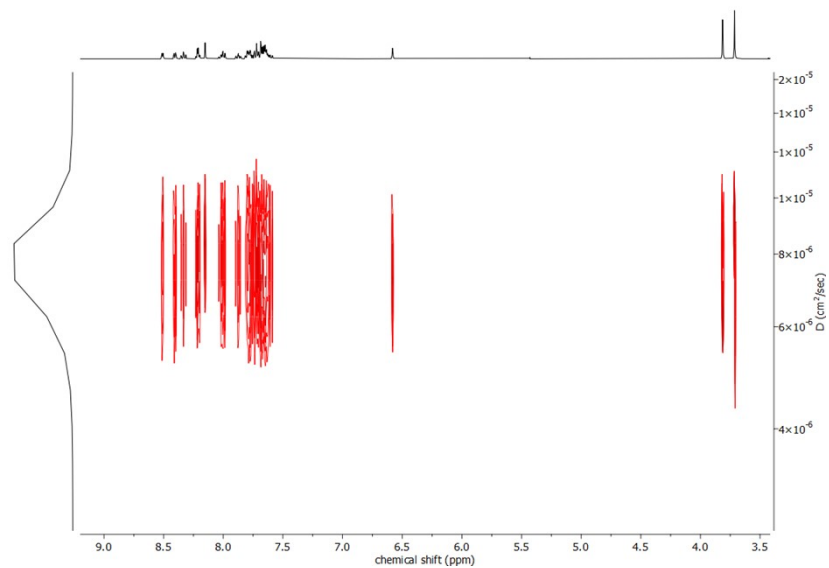


Figure S61. Plot of ^1H DOSY NMR experiment for determination of the diffusion coefficient of $[\text{Pd}_2(\mathbf{1})(\text{CH}_3\text{CN})_2](\text{OTf})_4$ (**2**) ($8.64 \text{ mmol}\cdot\text{L}^{-1}$, 25°C) in CD_3CN .

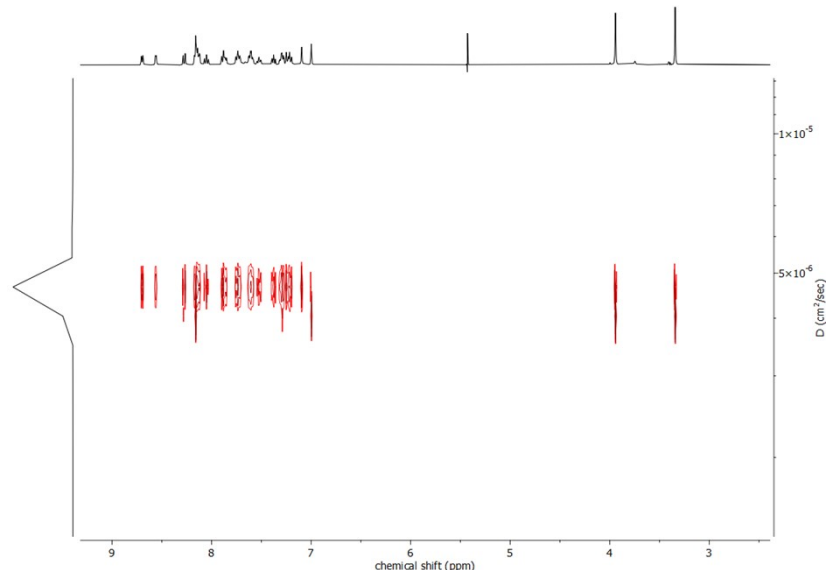


Figure S62. Plot of ^1H DOSY NMR experiment for determination of the diffusion coefficient of $[\text{Pd}(\mathbf{1})]_4(\text{OTf})_8$ (**3**) ($10.32 \text{ mmol}\cdot\text{L}^{-1}$, 25°C) in CD_3CN .

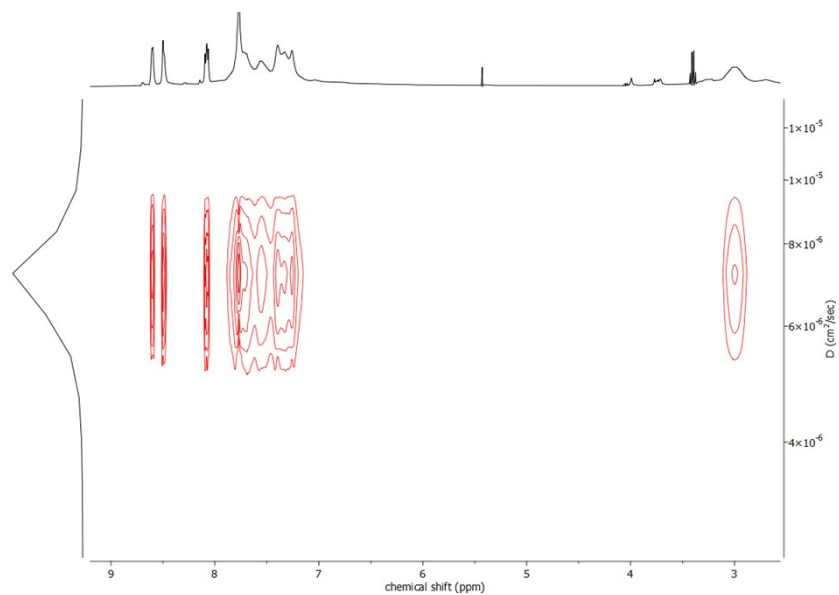


Figure S63. Plot of ¹H DOSY NMR experiment for determination of the diffusion coefficient of $[\text{Pd}(1)_2](\text{OTf})_2$ (**4**) ($9.17 \text{ mmol}\cdot\text{L}^{-1}$, 25°C) in CD_3CN .

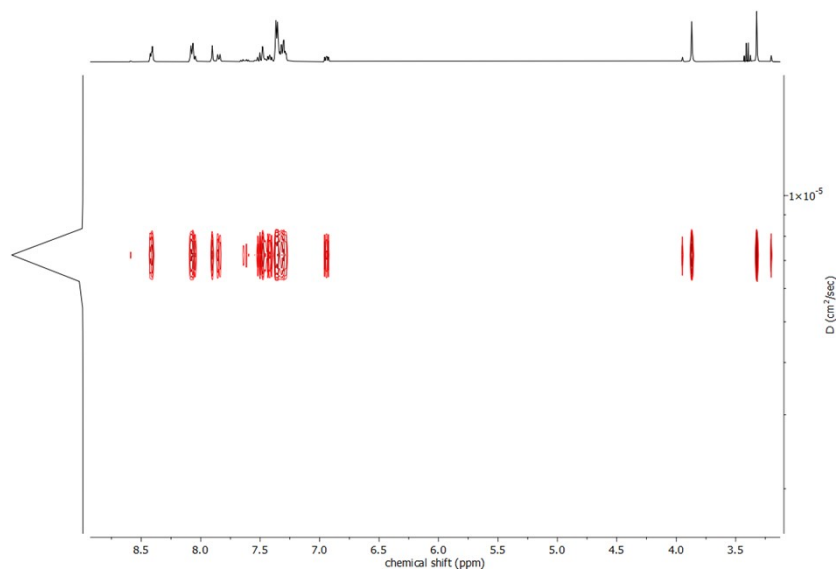


Figure S64. Plot of ¹H DOSY NMR experiment for determination of the diffusion coefficient of $[\text{Zn}(1)_2](\text{OTf})_2$ (**5**) ($8.83 \text{ mmol}\cdot\text{L}^{-1}$, 25°C) in CD_3CN .

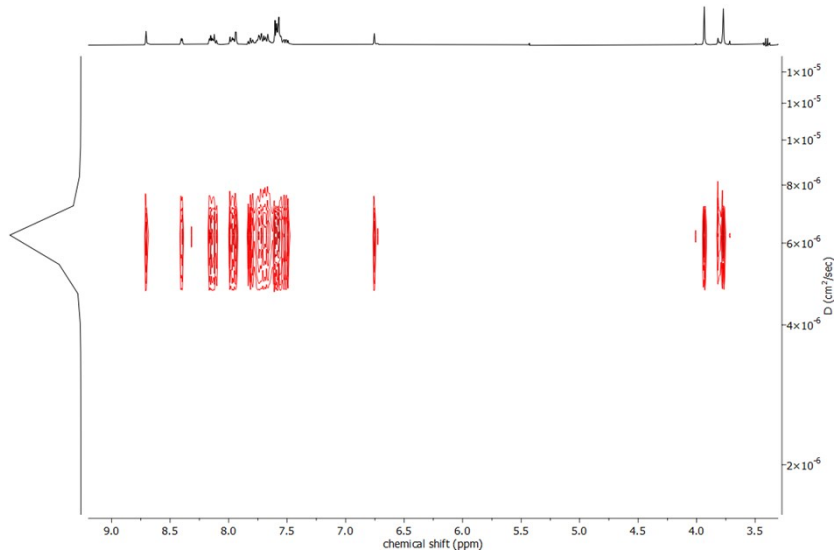


Figure S65. Plot of ¹H DOSY NMR experiment for determination of the diffusion coefficient of $[\text{Pd}_2\text{Zn}(1)_2](\text{OTf})_6$ (**6**) ($8.90 \text{ mmol}\cdot\text{L}^{-1}$, 25°C) in CD_3CN .

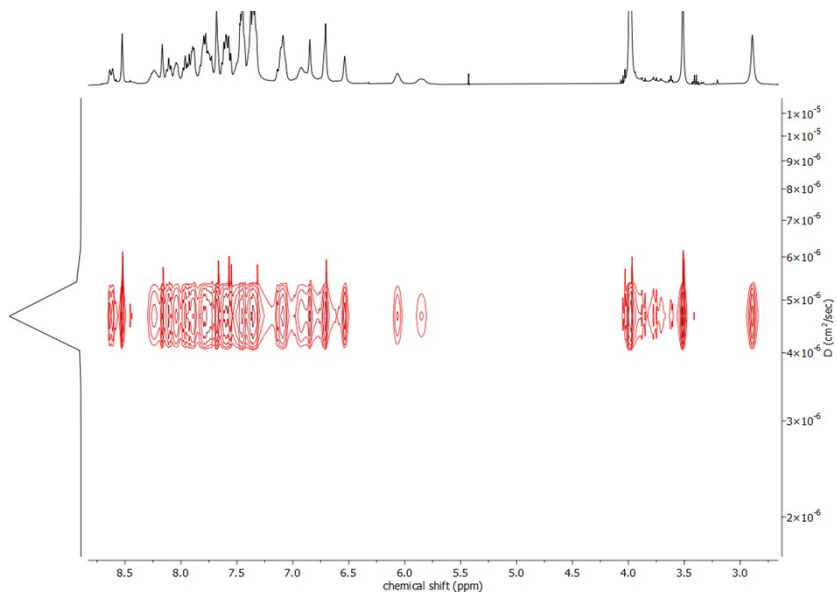


Figure S66. Plot of ¹H DOSY NMR experiment for determination of the diffusion coefficient of $[\text{Pd}_2\text{Zn}_2(1)_4](\text{OTf})_8$ (**7**) ($9.23 \text{ mmol}\cdot\text{L}^{-1}$, 25°C) in CD_3CN .

Table S1. Diffusion coefficients D for complexes **2–7** obtained by ^1H DOSY NMR spectroscopy (CD_3CN , 25 °C, concentration as indicated) by fitting the individual peaks' integral decay vs. the gradient strength applied. For comparability between the

Compound	Concentration (mmol · L ⁻¹)	Compound diffusion coefficient D [Complex]	D [TMS] (10 ⁻¹⁰ m ² · s ⁻¹)	D [CD_2HCN]
[Pd ₂ (1)(CH ₃ CN) ₂](OTf) ₄ (2)	8.64	7.70	28.3	36.0
[Pd(1) ₄ (OTf) ₈ (3)	10.32	4.51	26.9	34.4
[Pd(1) ₂](OTf) ₂ (4)	9.17	7.12	28.0	35.7
[Zn(1) ₂](OTf) ₂ (5)	8.83	7.18	28.1	35.6
[Pd ₂ Zn(1) ₂](OTf) ₆ (6)	8.90	6.21	27.7	35.1
[Pd ₂ Zn ₂ (1) ₂](OTf) ₈ (7)	9.23	4.79	26.8	33.6

individual measurements, diffusion coefficients D for CD₂HCN and tetramethylsilane (TMS) are also listed.

10. Mass Spectrometry

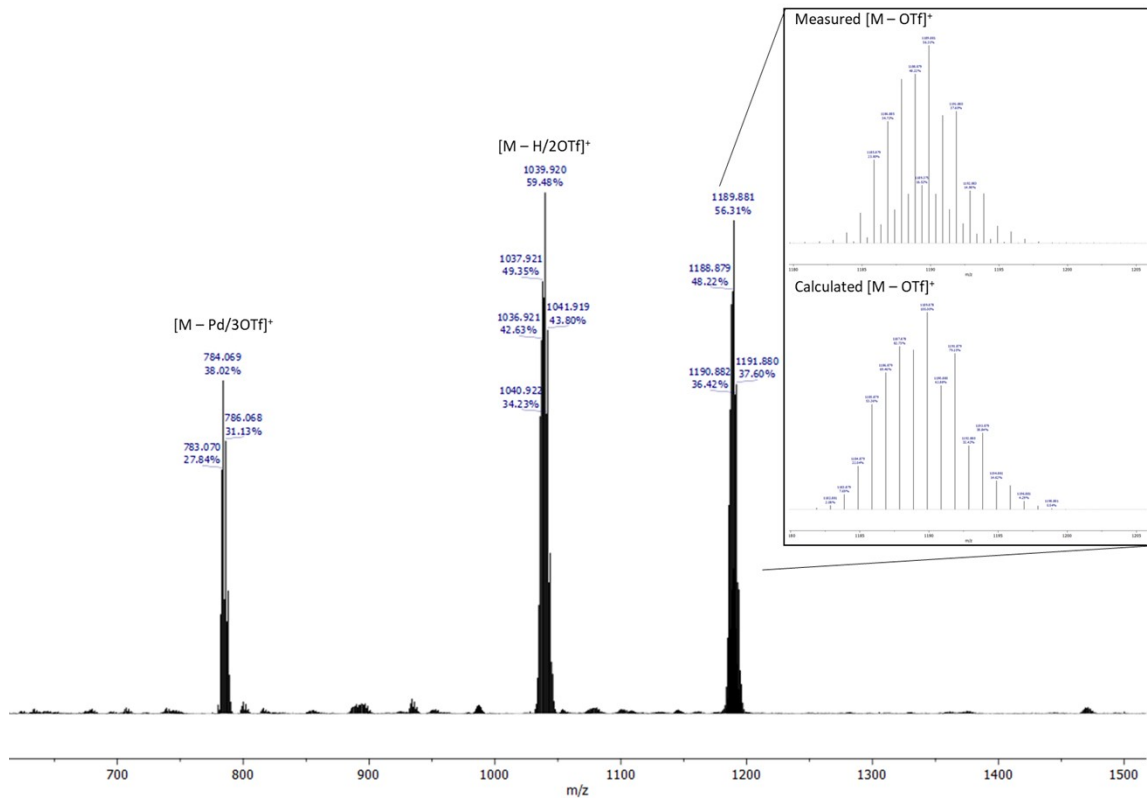


Figure S67. HR-ESI+ mass spectrum of [Pd₂(**1**)(CH₃CN)₂](OTf)₂ (**2**) in CH₃CN.

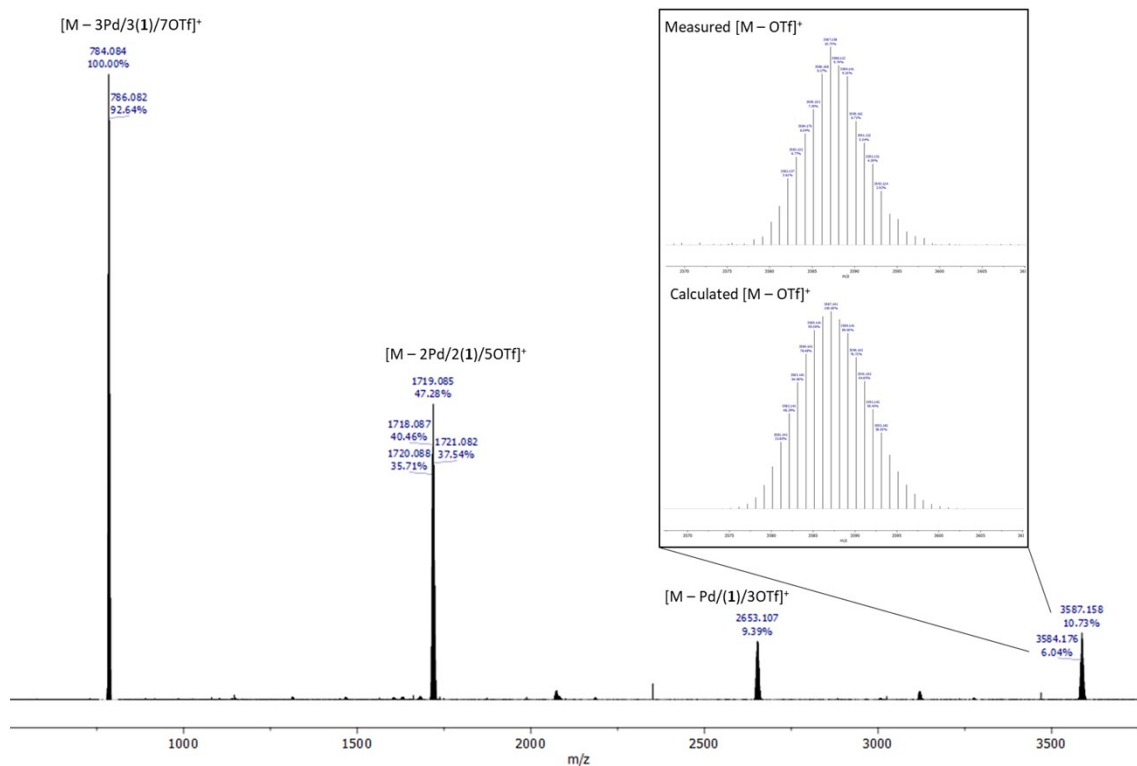


Figure S68. HR-ESI+ mass spectrum of $[\text{Pd}(\mathbf{1})_4](\text{OTf})_8$ (**3**) in CH_3CN .

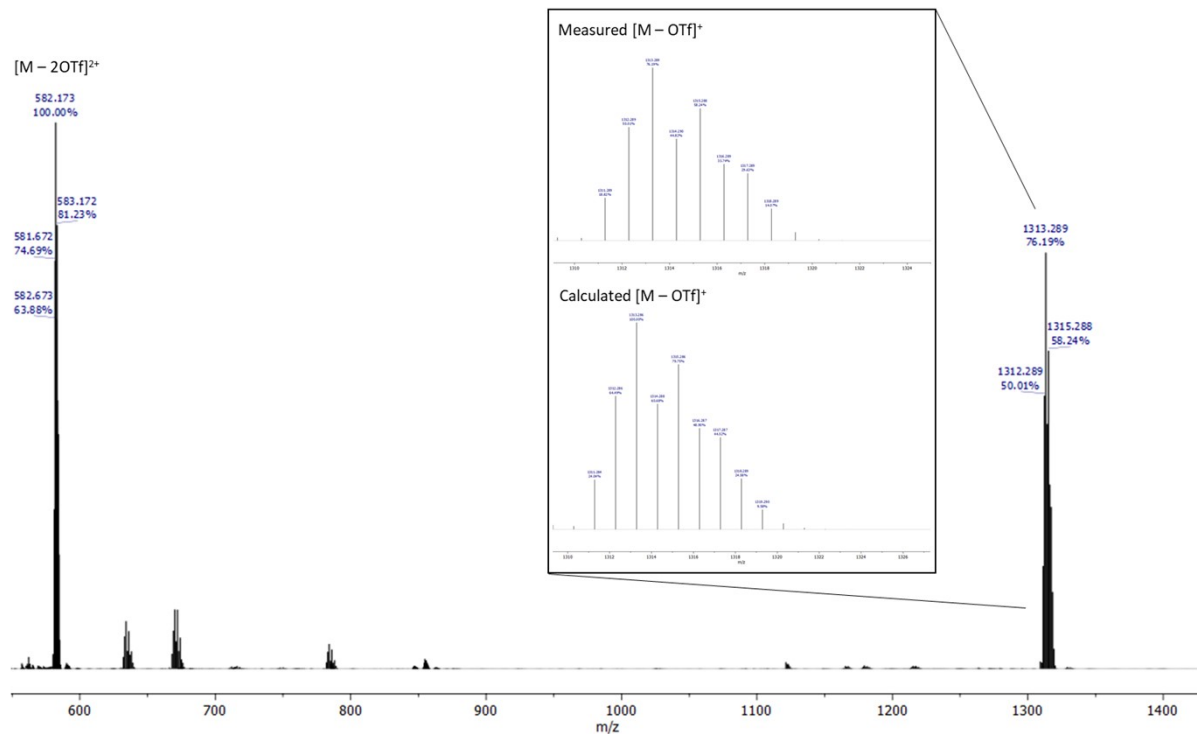


Figure S69. HR-ESI+ mass spectrum of $[\text{Pd}(\mathbf{1})_2](\text{OTf})_2$ (**4**) in CH_3CN .

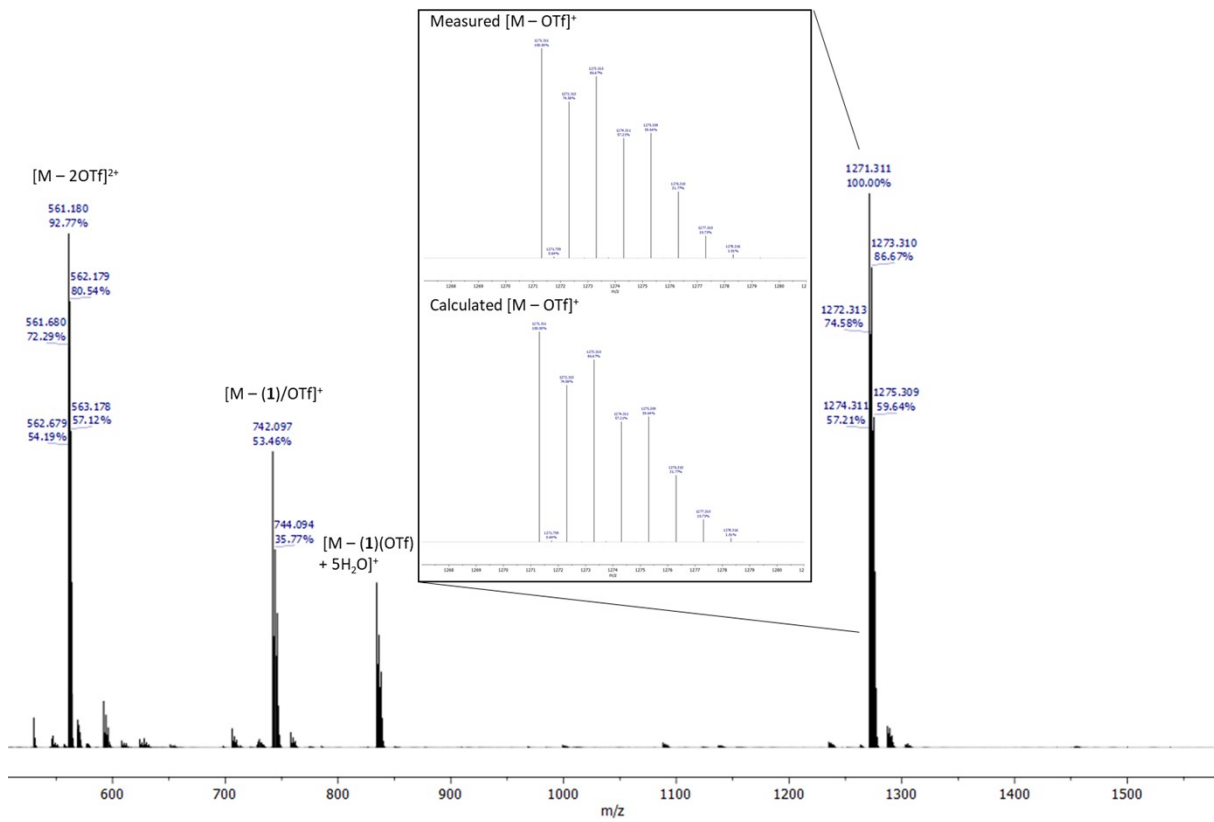


Figure S70. HR-ESI+ mass spectrum of $[\text{Zn}(\mathbf{1})_2](\text{OTf})_2$ (**5**) in CH_3CN .

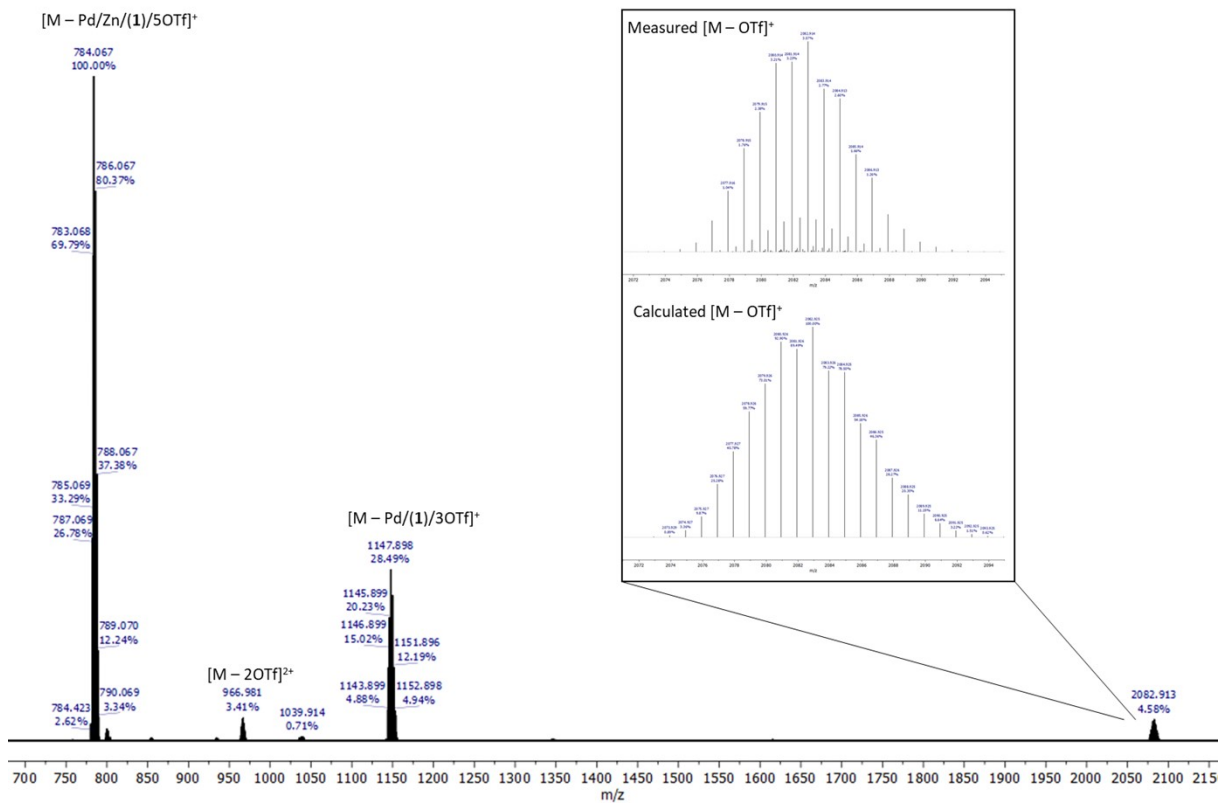


Figure S71. HR-ESI+ mass spectrum of $[\text{Pd}_2\text{Zn}(1)_2](\text{OTf})_6$ (**6**) in CH_3CN .

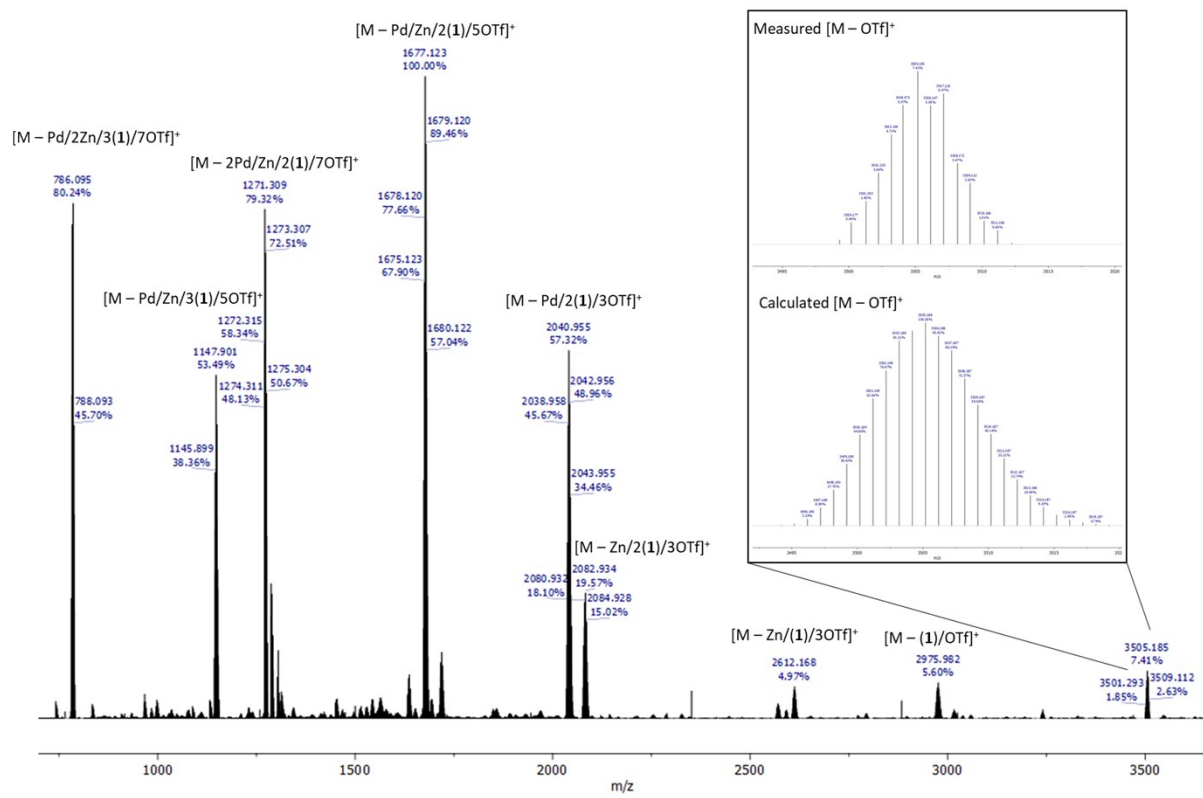


Figure S72. HR-ESI+ mass spectrum of $[\text{Pd}_2\text{Zn}_2(\mathbf{1})_4](\text{OTf})_8$ (**7**) in CH_3CN .

11. UV/Vis Spectroscopy

Compound	Solvent	Concentration ($\cdot 10^{-5}$ mol · L $^{-1}$)	Wavelength λ (nm)	Absorbance (a.u.)	Molar extinction coefficient ϵ (L · cm $^{-1}$ · mol $^{-1}$)
Ligand (1)	CH ₂ Cl ₂	2.9	230	1.366	27100
			286	0.857	17000
			318	1.128	22400
			346	1.095	21700
[Pd ₂ (1)(CH ₃ CN) ₂](OTf) ₄ (2)	CH ₃ CN	2.6	253	0.843	32200
			293 ¹	0.526	20100
			397 ¹	0.802	30700
			416	1.006	38500
[Pd(1)] ₄ (OTf) ₈ (3)	CH ₃ CN	2.0	235	1.422	72400
			276	0.816	41600
			331	1.074	54700
			373	1.026	52300
[Pd(1) ₂](OTf) ₂ (4)	CH ₃ CN	2.3	230	0.970	42600
			285	0.536	23500
			331	0.743	32600
			358 ¹	0.607	26700
[Zn(1) ₂](OTf) ₂ (5)	CH ₃ CN	2.5	270	0.676	27000
			373	1.380	55100
			234	1.104	29600
			273 ¹	0.734	19700
[Pd ₂ Zn(1) ₂](OTf) ₆ (6)	CH ₃ CN	3.7	333 ¹	0.715	19100
			382	1.082	29000
			231	1.029	14100
			266	0.744	10200
[Pd ₂ Zn ₂ (1) ₄](OTf) ₈ (7)	CH ₃ CN	0.7	332 ¹	0.682	18200
			375	1.328	93500

Table S2. UV/Vis data of compounds **1–8**.

¹ Shoulder.

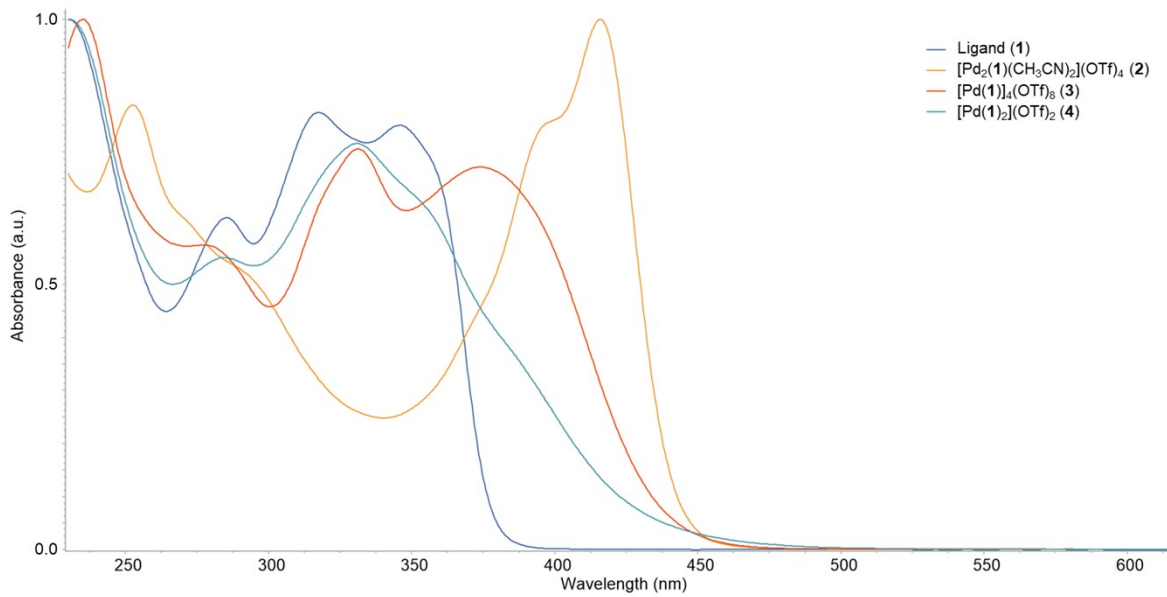


Figure S73. UV/Vis spectra of ligand (1) (in CH_2Cl_2) and complexes **2**–**4** (in CH_3CN).

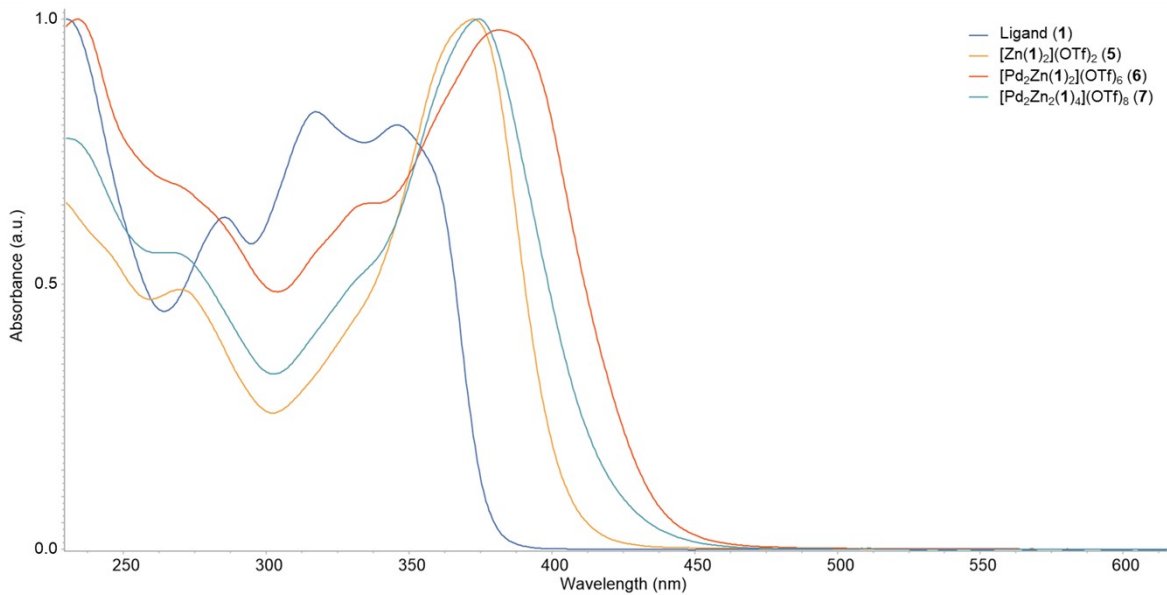


Figure S74. UV/Vis spectra of ligand (1) (in CH_2Cl_2) and complexes **5**–**7** (in CH_3CN).

12. Additional Information on X-Ray Diffraction Analyses

Table S3. Summary of crystallographic data.

Compound	2·2CH ₃ CN	3·4CH ₃ CN ·CH ₂ Cl ₂ ^[1]	4·5CH ₂ Cl ₂	7·6CH ₃ CN ·6CH ₂ Cl ₂
Empirical formula	C ₄₃ H ₄₀ F ₁₂ N ₁₁ O ₁₂ PPd ₂ S ₄	C ₁₄₁ H ₁₂₄ Cl ₂ F ₂₄ N ₃₂ O ₂₄ P ₄ Pd ₂ S ₈	C ₆₉ H ₆₆ Cl ₁₀ F ₆ N ₁₄ O ₆ P ₂ PdS ₂	C ₁₅₀ H ₁₄₂ Cl ₁₂ F ₂₄ N ₃₄ O ₂₄ P ₄ Pd ₂ S ₈ Zn ₂
Formula weight	1502.87	3983.57	1888.31	4410.27
T/K	130	130	130	180
λ/Å	0.71073	0.71073	0.71073	1.54186
Crystal system	Monoclinic	Monoclinic	Monoclinic	Monoclinic
Space group	C2/c	P2 ₁ /c	P2 ₁ /n	P2 ₁ /c
a/Å	23.1345(3)	26.4899(3)	13.9015(1)	18.2836(3)
b/Å	19.3453(2)	21.7388(3)	38.1339(4)	25.6217(3)
c/Å	50.1762(6)	32.7073(3)	14.9542(2)	39.2969(6)
α/°	90	90	90	90
β/°	94.366(1)	95.369(1)	98.185(1)	96.946(1)
γ/°	90	90	90	90
V/Å ³	22390.9(5)	18752.1(4)	7846.7(2)	18273.8(5)
Z	16	4	4	4
ρ _{calcd.} /g·cm ⁻³	1.783	1.411	1.598	1.603
μ/mm ⁻¹	0.929	0.619	0.746	5.513
F(000)	12000	8032	3832	8928
Crystal size/mm ³	0.050 x 0.150 x 0.150	0.250 x 0.400 x 0.400	0.300 x 0.300 x 0.400	0.050 x 0.200 x 0.250
Colour and shape	Yellow plate	Yellow prism	Orange prism	Yellow plate
θ _{max} /°	27.344	27.367	28.033	68.000
GooF on F ²	1.055	1.025	1.092	1.023
R _{int} /%	5.59	6.89	4.62	5.64
R ₁ /wR2 (I>2σ)/%	5.99/13.36	5.58/13.81	6.11/13.69	9.26/24.68
R ₁ /wR2 (all data)/%	7.93/14.28	8.82/15.38	7.87/14.58	12.18/27.92
Largest diff. peak/hole/e·Å ⁻³	1.663/-0.708	1.325/-1.595	1.213/-0.875	1.660/-1.173

^[1] The large unit cell of 3·4CH₃CN·CH₂Cl₂ contained a high number of solvent molecules and a highly disordered triflate in the asymmetric unit, which could not be resolved sufficiently with a reasonable accuracy. A significant unidentified high number of dichloromethane (CH₂Cl₂) and acetonitrile molecules (CH₃CN) was removed by the SQUEEZE procedure. Consequently, the exact amount of lattice solvent molecules was not determinable.

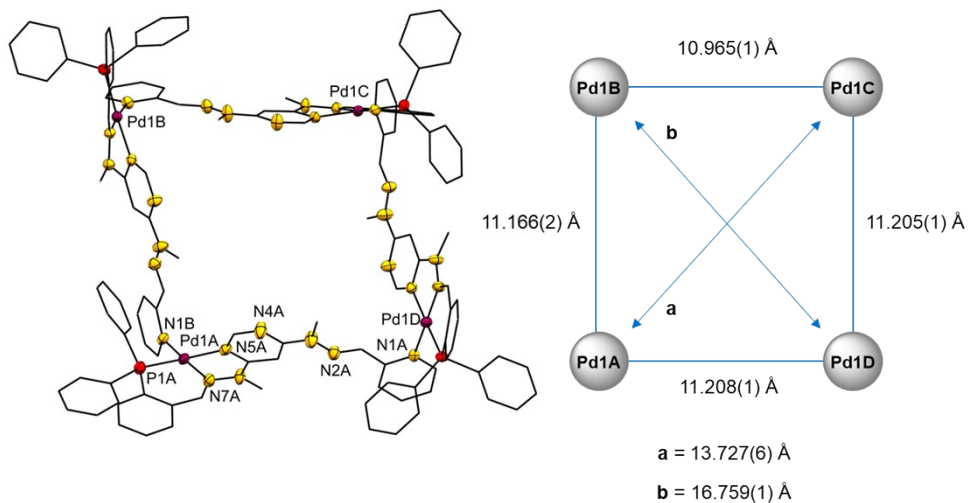


Figure S75. Molecular structure of **3**·4CH₃CN·CH₂Cl₂ and intermetallic Pd···Pd distances in the rectangular macrocycle (triflate anions, solvent molecules and hydrogen atoms are omitted, carbon atoms are drawn as wireframes and **3** includes non-symmetry related A–D labels for clarity; thermal ellipsoids are set at the 50% probability level).

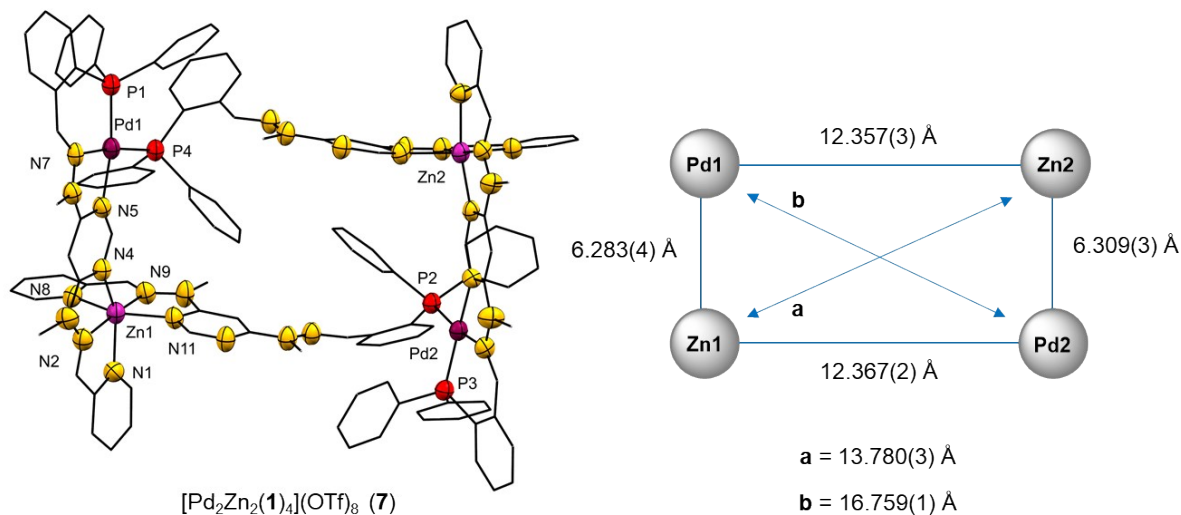


Figure S76. Molecular structure of **7**·6CH₃CN·6CH₂Cl₂ and intermetallic Pd···Pd distances in the rectangular macrocycle (triflate anions, solvent molecules and hydrogen atoms are omitted, and carbon atoms are drawn as wireframes for clarity; thermal ellipsoids are set at the 50% probability level).